HERA-ZEUS Document
Oct-22-1999

A Luminosity Spectrometer for ZEUS

A. Caldwell, S. Paganis, R. Sacchi, F. Sciulli

Columbia University, Nevis Laboratories,
P.O.Box 137, Irvington, NY 10533

Abstract

The HERA luminosity upgrade is expected to generate two major problems in the current method of luminosity determination which is based on counting brehmsstrahlung photons: damage of the calorimeter monitor due to high primary synchrotron radiation and large multiple event (pile-up) corrections. The proposed luminosity spectrometer reduces the impact of these problems in the luminosity measurement, yielding a total systematic error in the order of 1%. The spectrometer counts brehmsstrahlung photon conversions in the beam pipe exit window using two small calorimeters symmetrically placed away from the synchrotron radiation plane XZ. The photon conversion rate is measured by counting electron-positron coincidences in the calorimeters. The electron-positron pair is separated by a small dipole magnet.

Contents

1 Introduction

In this note an alternative technique for measuring luminosity in ZEUS after the HERA luminosity upgrade [1] is presented. The luminosity is still determined via measurement of the rate of the bremsstrahlung process $ep \to ep\gamma$ [2]. The measurement is performed by counting the bremsstrahlung photons which leave the beam pipe window about 92 m from the interaction point (IP). The beam pipe window is assumed to be 5cm radius and 3mm thickness (90% Cu, 10% Be) converting $\simeq 11\%$ ($E_\gamma \simeq 20GeV$) of the photons to e^+e^-. The coincidence rate is measured in a pair of small calorimeters placed downstream of a dipole magnet, to separate the e^+e^- pair (see fig 2). This rate is proportional to the luminosity:

$$L = \frac{Rate}{(Acceptance) \times (\sigma_{ep\to ep\gamma})}. \tag{1}$$

Thus, knowledge of the acceptance and the calculated cross section yields the luminosity.

Before we proceed with the detailed description of the technique, we list the main characteristics obtained from this study.

- Small systematic errors due to pile-up. With acceptance $A \simeq 3\%$, the chances of confusion from a second photon are reduced by two orders of magnitude.
- Accurate knowledge of the acceptance ($\Delta A/A < 1\%$) in a window of width $\Delta E_\gamma \simeq 3\ GeV$, as determined with the use of the 6m tagger.
- Insensitive to synchrotron radiation even at peak luminosity.
- Small errors from energy scale uncertainty due to the good BPC resolution (single photon energy measurement resolution is of order 3-4%), absence of pile-up, and the beam energy constraint.
- The measured coincidence rates 3 KHz for $L = 10^{31}cm^{-2}s^{-1}$ allow for independent sequential measurements of the luminosity and monitoring of beam changes every few seconds.
- Good photon beam profile reconstruction at the exit window. Shifts of the profile mean values smaller than $\simeq 2mm$ can be measured every 10 seconds. The standard deviation of the profile distribution can be reconstructed with a few % uncertainty.
- The theoretical photon bremsstrahlung cross section is well understood in the energy range used by the spectrometer.

We believe that these characteristics make the technique much simpler and more accurate than the current luminosity measurement method, especially for high luminosity operation after the HERA upgrade.

We have chosen for the two calorimeters the existing beam pipe calorimeters (BPC). In this note we will refer to this setup as the lumi spectrometer. The spectrometer, with resolution $\sigma/E = 0.17/\sqrt{E}$ can measure the rate of converted photons with a small systematic error (below 1%). On the other hand the acceptance (when we fold conversion) is around 3% which means that a correction factor of 33 is needed. This correction factor has to be known with an accuracy of better than 1% in order to meet the requirements of ZEUS physics. The correction factor for the spectrometer acceptance can be obtained by Monte-Carlo simulations, measurement of the beam profile, beam angle etc. Unfortunately the error involved with this technique is at least 5% to 10%. Instead, the use of an independent device that "tags" the bremsstrahlung photons will provide a more accurate determination of the spectrometer acceptance. This device needs to have high and well known acceptance for bremsstrahlung electrons in the energy window which corresponds to the expected photon energy range of interest. We assume the simultaneous operation of the planned *6 meter tagger* located 6 meters from the interaction point [3].

The well understood BPC energy resolution and linearity allow the photon spectrum end point ($\simeq 27.5\ GeV$) to be used for both the calorimeter energy calibration and the 6m tagger calibration. A small uncertainty exists within the energy window boundaries for which coincidences between the two devices are measured ($\simeq 0.5\%$). So long as the 6m tagger has high acceptance for bremsstrahlung electrons (and small and measured contamination), the acceptance correction factor should also be known with an accuracy of order 1.0%.

In this note the spectrometer method is presented and the associated systematic errors are estimated. The longitudinal position of and the transverse distance between the two calorimeters used in this study could change without changing the final conclusions, since the magnetic field $\int BdL$ can be adjusted to compensate. Overall the method is expected to give a luminosity measurement with an accuracy better than 1.4%.

This proposal only concerns itself with the details and operation of the spectrometer. The electronic readout and DAQ is discussed in a separate document [4].

2 Measuring the ZEUS Luminosity

The instantaneous luminosity of ZEUS is measured using the formula:

$$L = \frac{R}{\sigma} \tag{2}$$

where R is the corrected rate of $ep \to ep\gamma$ bremsstrahlung events within a specified photon energy window (E_1 to E_2), and σ is the calculated cross-section within the same window.

The corrected rate is found from the spectrometer coincidence rate R_0 as follows:

1. A correction for *egas* background interactions [2] is applied:

$$R_1 = R_0 - \frac{I_e^{tot}}{I_e^{pilot}} R^{pilot} \tag{3}$$

where I_e^{tot} is the total colliding bunch electron current, and I_e^{pilot} the electron current of the pilot bunches.

2. An acceptance correction is applied:

$$R_2 = \frac{R_1}{\overline{a}(x_0, y_0, \sigma_x, \sigma_y)} \tag{4}$$

where $\overline{a}$ is the average acceptance calculated from coincidence data of the luminosity spectrometer with the 6 meter tagger (see fig. 1). The acceptance will depend on the measured values of $x_0, y_0, \sigma_x, \sigma_y$ which are the gaussian means and standard deviations of the photon profile in the transverse plane. The average acceptance $\overline{a}$ is given by the corrected measured acceptance $\overline{a}'$:

$$\overline{a} = C\overline{a}' = C\frac{N_{coinc}^{CORRECTED}}{N_{tags}^{CORRECTED}} \tag{5}$$

where C is a correction factor and the corrected number of coincidences $N_{coinc}^{CORRECTED}$ and tags $N_{tags}^{CORRECTED}$ are:

$$N_{coinc}^{CORRECTED} = N_{coinc}^{MEAS} - N_{coinc}^{PILEUP} - N_{coinc}^{EGAS} \tag{6}$$
$$N_{tags}^{CORRECTED} = N_{tags}^{MEAS} - N_{tags}^{OFFMOM} - N_{tags}^{EGAS}. \tag{7}$$

These corrections include multiple event subtraction (N^{PILEUP}), *egas* event subtaction (N^{EGAS}) and off momentum electron event subtraction for the 6 meter tagger (N^{OFFMOM}). The correction factor C accounts for the 6 meter tagger energy scale and linearity uncertainties and the possibly different energy window used for acceptance calculations and luminosity measurement. C is expected to be close to 1.

3. Multiple events (pile-up) correction is applied:

$$R = f(R_2)R_2 \ , \tag{8}$$

where $f(R_2)$ is the rate dependent correction factor for pile-up which is obtained from calculation.

As a final step one needs the calculated cross-section within the bremsstrahlung photon energy window using the theoretical Bethe-Heitler formula:

$$\sigma = \int_{E_1}^{E_2} \frac{d\sigma^{BH}}{dE_\gamma} \otimes g(E_\gamma) dE_\gamma \tag{9}$$

where $g(E_\gamma)$ is the BPC detector response function convoluted with the theoretical cross section density.

The calculated 6 meter tagger acceptance is shown in figure 1 [3].

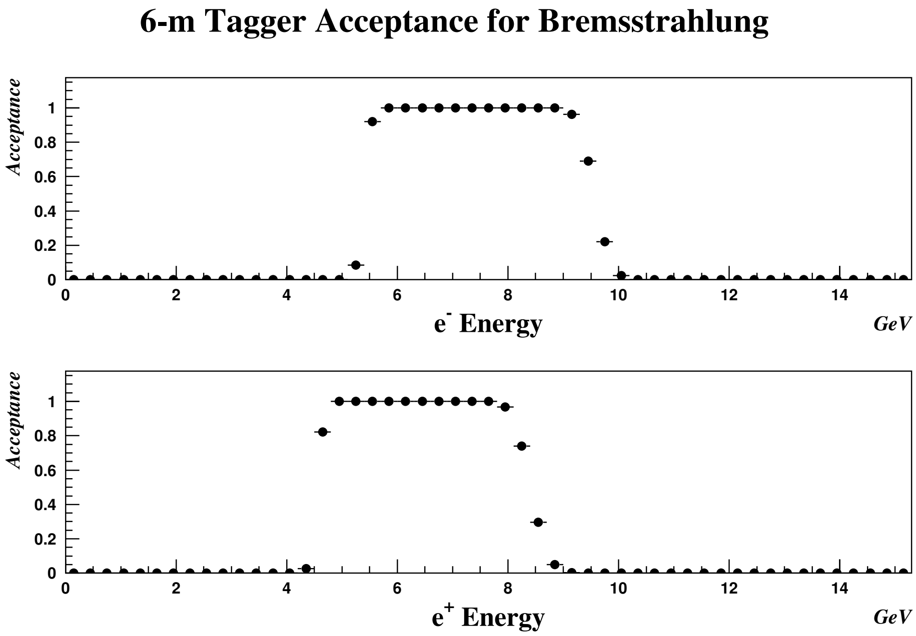

Figure 1: Acceptance of the 6m tagger exit window for bremsstrahlung electrons (top) and positrons (bottom). The acceptance is $> 99\%$ over the ranges $6 - 9GeV$ for e^- and $5 - 8GeV$ for e^+.

3 Spectrometer Experimental Layout and Optimizations

The proposed luminosity spectrometer experimental setup is shown if figure 2. In this figure the photon beam pipe window is located 92m downstream the IP, a 60cm long (along Z) dipole magnet is placed a few cm downstream of the window and finally the 2 beam pipe calorimeters are placed 9.8m downstream of the window. The calorimeters are positioned off the XZ plane because this is the synchrotron radiation plane. In fig. 3 the AB cut is shown (XY plane). The cylinder on the top of the figure is the proton beam pipe.

The spectrometer acceptance A is given by the formula:

$$A = A_{geom} \cdot A_{conv} \cdot A_z \tag{10}$$

where A_{geom} is the acceptance of the photon beam exit window (it is of order 90-95%), A_{conv} is the conversion rate (for the specific exit window this is $A_{conv} \simeq 10\%$), and A_z describes the $z = E_e/E_\gamma$ dependent part of the acceptance. In most of the following plots the conversion factor A_{conv} was omitted for simplicity (for different

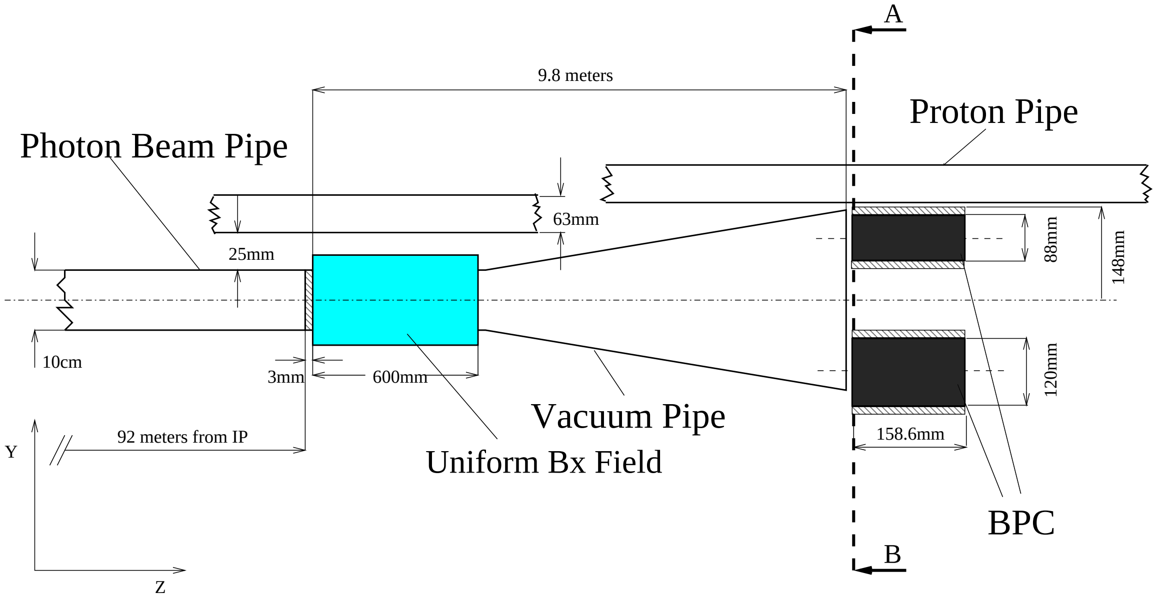

Figure 2: Experimental layout of the luminosity spectrometer for ZEUS.

window designs the results of this study have to be multiplied by the new conversion factor).

The positions of the BPC were varied in order to optimize the e^+e^- acceptance. A minimum separation of 10 cm between the two calorimeters was required in order to avoid direct photon hits. The criteria of this optimization are:

- achieve the highest possible BPC acceptance for e^+e^- conversions of interest.
- achieve maximum uniformity of the BPC acceptance over a 10 GeV energy window.

The results of the Monte Carlo simulation performed using the Geant3.2 package are shown in figure 4. In this plot comparison between the optimum case with various other cases is presented. The optimum case is the curve with the empty triangle markers present in every plot. The optimum BPC position found, is at 9.8m downstream the exit window for $\int BdL = 0.5 \times 0.6T \cdot m$.

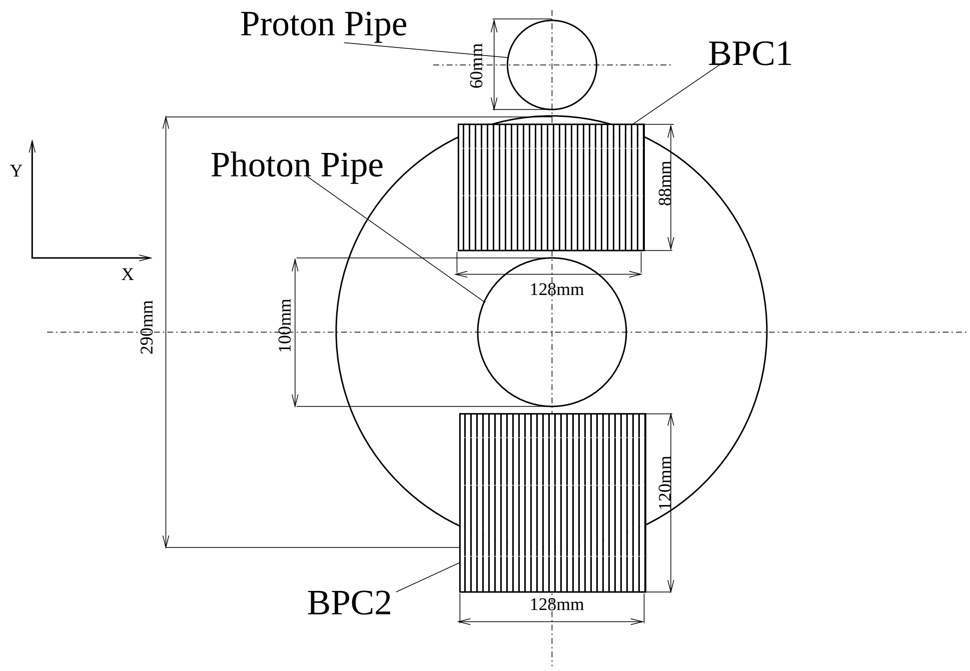

Figure 3: AB section view of spectrometer layout. Only the active volume of the BPC modules is shown. There are three 5 mm thick tungsten bars around this volume, two of them in the top and bottom making the total small BPC height 98 mm.

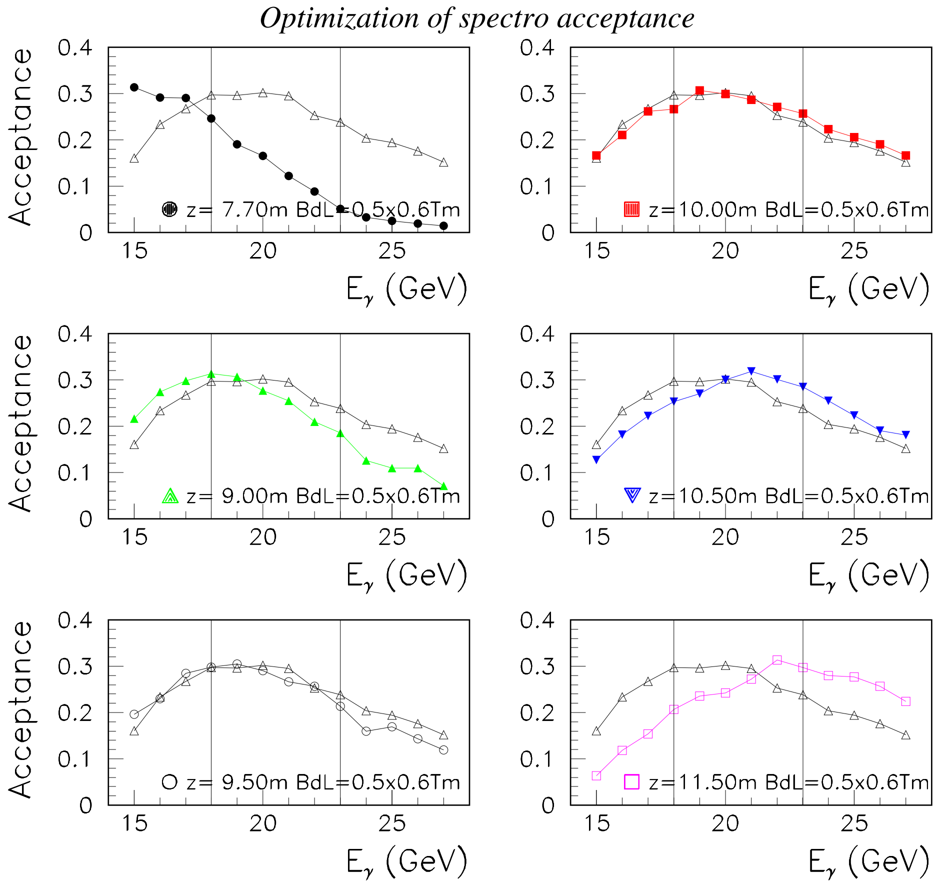

Figure 4: Acceptance optimization studies (conversion factor was omitted for simplicity).

4 Spectrometer performance

In this section the spectrometer performance is discussed. The spectrometer acceptance is found to be fairly flat within a photon energy window of width 5 GeV. The acceptance dependence on $z = E_e/E_\gamma$ is presented. The spectrometer is found to have over 99% acceptance in symmetric conversions within a z window ($z = 0.5 \pm 0.2$).

One of the big advantages of the spectrometer technique, is the high precision measurement of the photon energy distribution end-point ($\simeq 27.5\ GeV$). The measured photon energy spectrum by the spectrometer at the end-point region is presented.

Photon beam position and distribution variations occur with time, so that monitoring of these conditions is required. The spectrometer rates allow for monitoring every few seconds of running. Although during such short times no significant change in the running conditions is expected, if the luminosity runs are performed at times different than the acceptance runs, then one will have to correct for these changes. The spectrometer sensitivity in the BPC fiducial volume, beam position and distribution at the exit window, and in variations in the magnetic field is calculated.

In this section the single electron, single coincidence and multiple event (pile-up) rates are calculated for lower and peak specific luminosity. Finally the photon beam profile reconstruction using the luminosity spectrometer is discussed. It is found that the spectrometer sensitivity in photon beam profile shifts at the exit window, is better than $2mm$.

4.1 Spectrometer acceptance

The spectrometer acceptance for the optimum configuration is shown in figure 5. The e^+e^- coincidence acceptance is relatively uniform in the 18-23 GeV photon energy window. As it will be shown later, when the photon acceptance is flat, the uncertainty in the acceptance correction factor is minimum, thus minimizing the corresponding acceptance systematic error.

4.1.1 Acceptance $z = E_e/E_\gamma$ dependence

The y-distribution of the hits produced in the BPC by e^+e^- pairs from photon conversion and four different photon momentum bins, is represented by the shaded histograms shown in fig. 6. The full histograms show all hits in the BPC.

The $z = E_e/E_\gamma$ distribution of the same four photon momentum bins is shown in fig. 7. The shaded histogram shows the e^+e^- BPC coincidence distribution while the full histogram shows all conversions and the dashed histogram shows the single hits in the spectrometer. From these plots we can see that there is a portion of single hits in low $|y|$ values. As we will see from the next plot, these hits come from highly asymmetric conversions.

In figure 8, the two BPC module hit distribution is shown for symmetric decays $0.4 \leq z \leq 0.6$ and two different photon momenta (18 and 19 GeV).

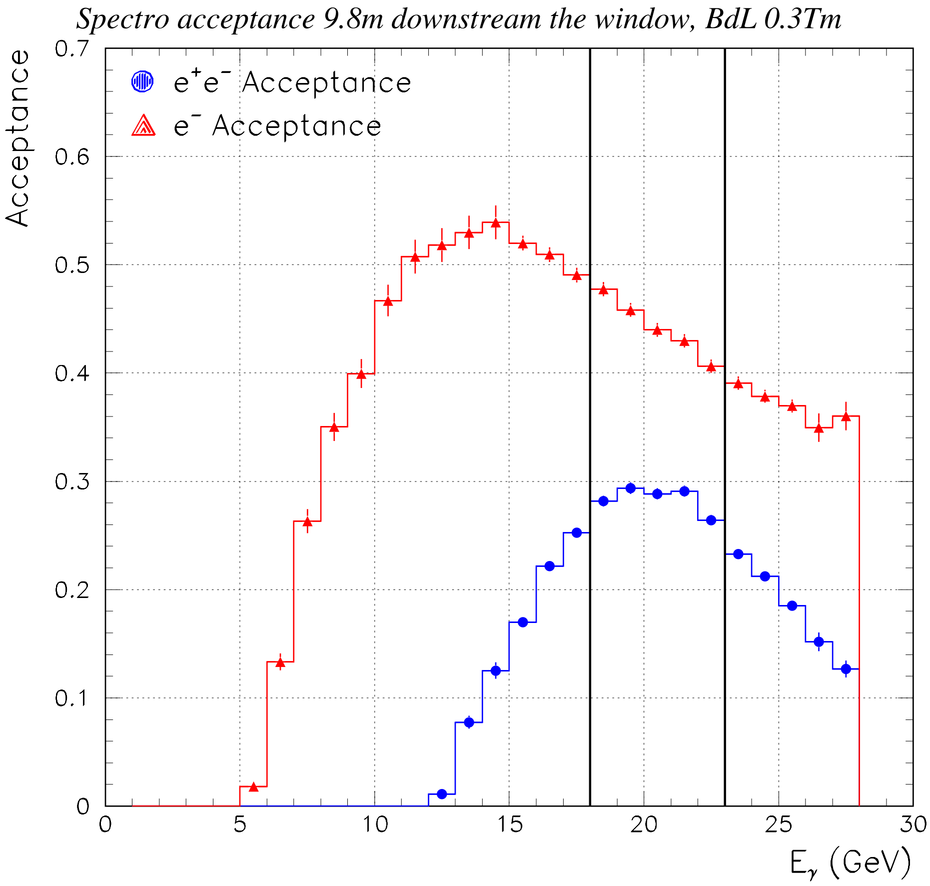

Figure 5: Acceptance for optimum configuration (conversion factor was omitted for simplicity).

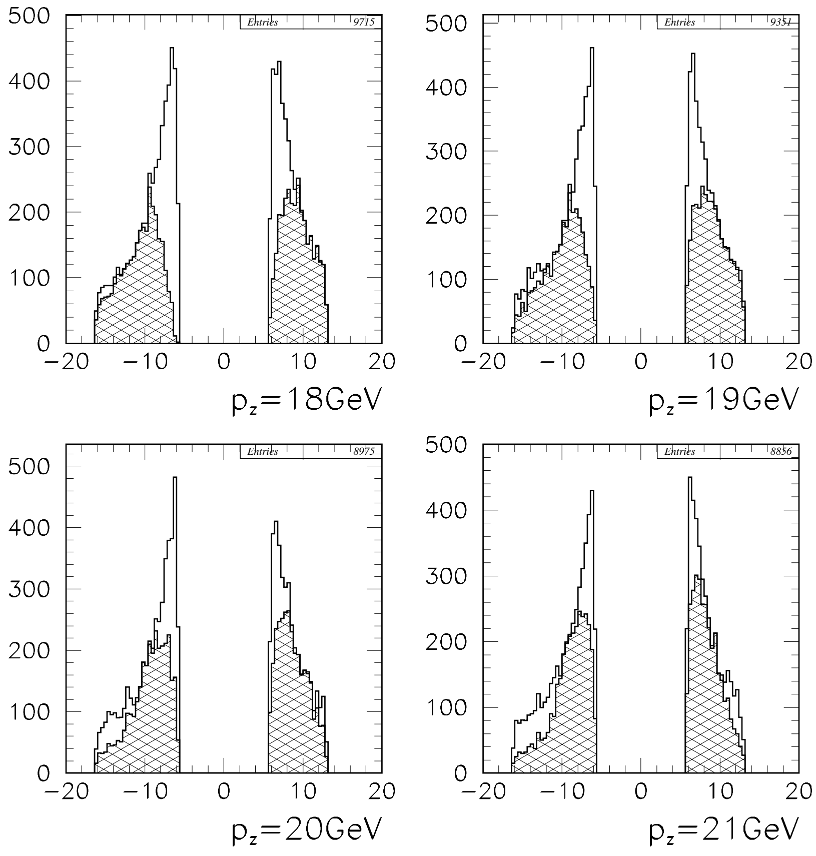

Figure 6: Y-distribution (in cm) of the hits produced in the BPC by e^+e^- pairs (shaded histograms) from photon conversion and four different photon momentum bins. The full histograms show all hits in the BPC.

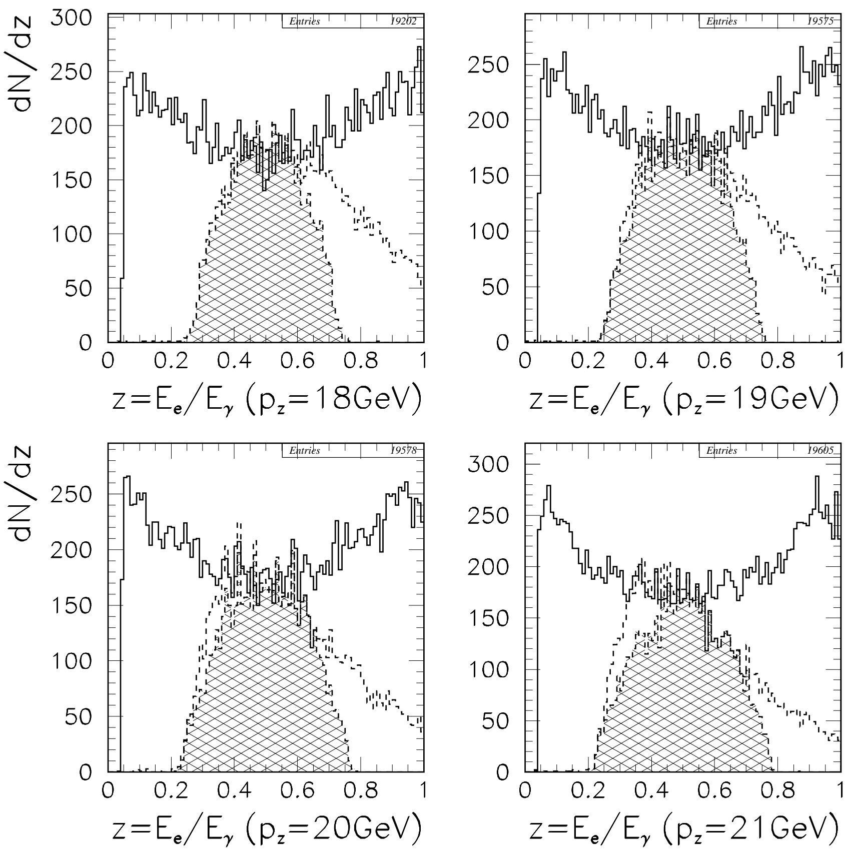

Figure 7: $z = E_e/E_\gamma$ distribution of four photon momentum bins. The shaded histogram shows the e^+e^- spectrometer coincidence distribution, the full histogram shows all conversions and the dashed histogram shows the single hits in the spectrometer.

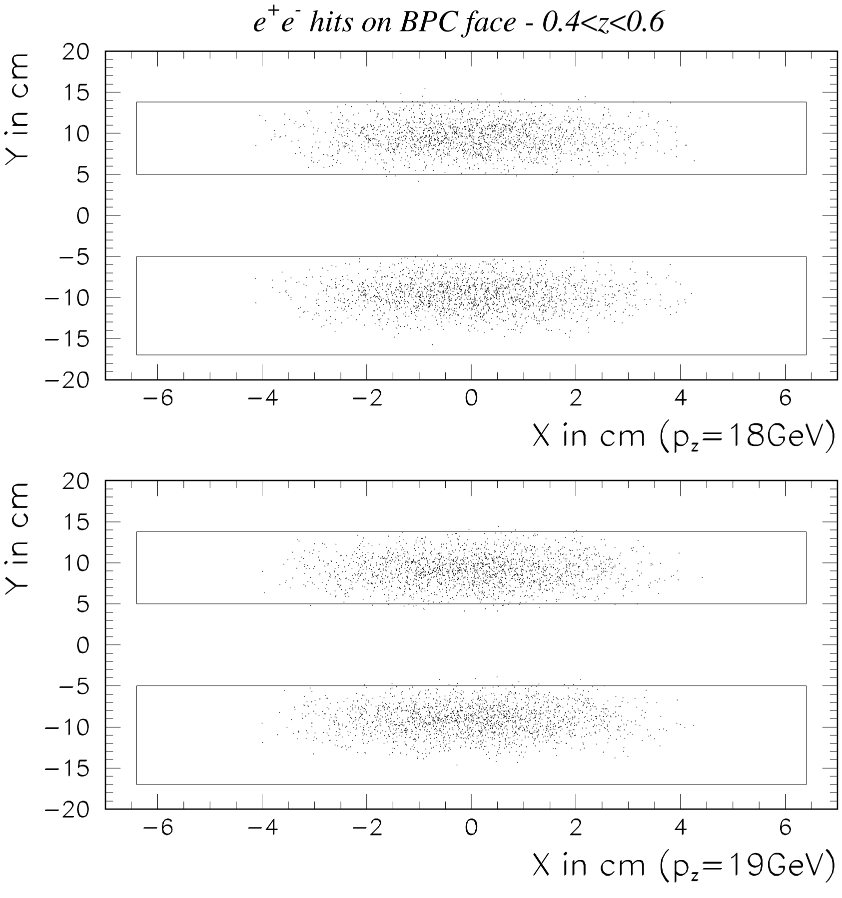

Figure 8: Hit distribution in the two BPC modules fiducial volumes for symmetric decays $0.4 \le z \le 0.6$ and two different photon momenta (18 and 19 GeV).

4.2 Measurement of the end-point of the photon spectrum

One of the big advantages of the spectrometer method in measuring the ZEUS luminosity, is its ability to measure with high accuracy the end-point ($\simeq 27.5\ GeV$) of the photon energy spectrum. Accurate measurement of the end-point provides energy calibration for the spectrometer.

The spectrometer acceptance as shown in fig. 5, falls rapidly with respect to the photon energy in the area of the spectrum end-point. An increase of the $\int BdL$ by 20-25% effectively shifts the relatively flat part of the acceptance to higher energies. A full simulation was performed with a 20% increase in the magnetic field and with realistic spectrometer resolution, to determine the sensitivity in the measurement of the end-point. The spectrometer acceptance for $\int BdL = 0.36Tm$ is shown in fig. 9. In fig. 10 the 10% of the initial spectrum is shown (thick full line), the spectrum

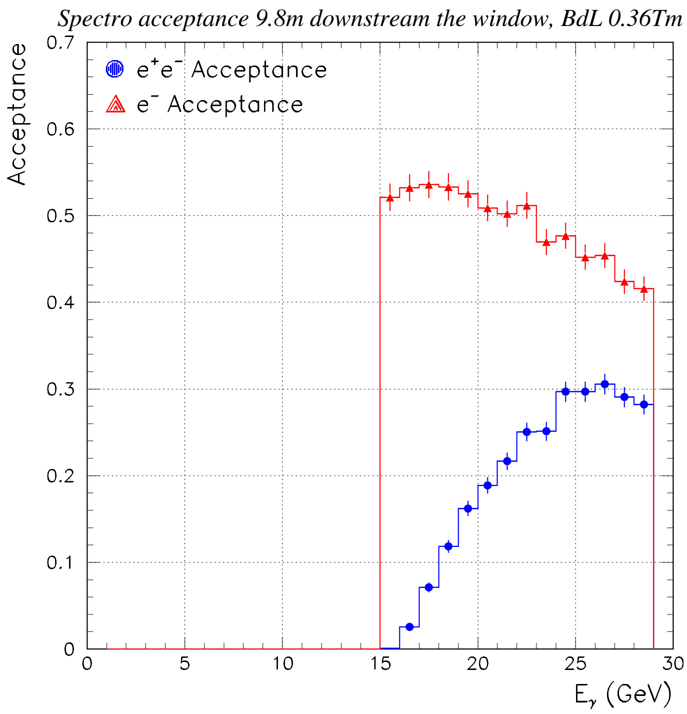

Figure 9: Spectrometer acceptance for $\int BdL = 0.36Tm$ as a function of the converted photon energy.

of the coincidences in the spectrometer acceptance without any detector resolution (thin full line) and the spectrum of the coincidences in the acceptance with detector resolution folded (dashed line). In this figure the sharp fall of the MC spectrum can be seen, while the smearing of the end-point position due to the spectrometer resolution is also shown (dashed line).

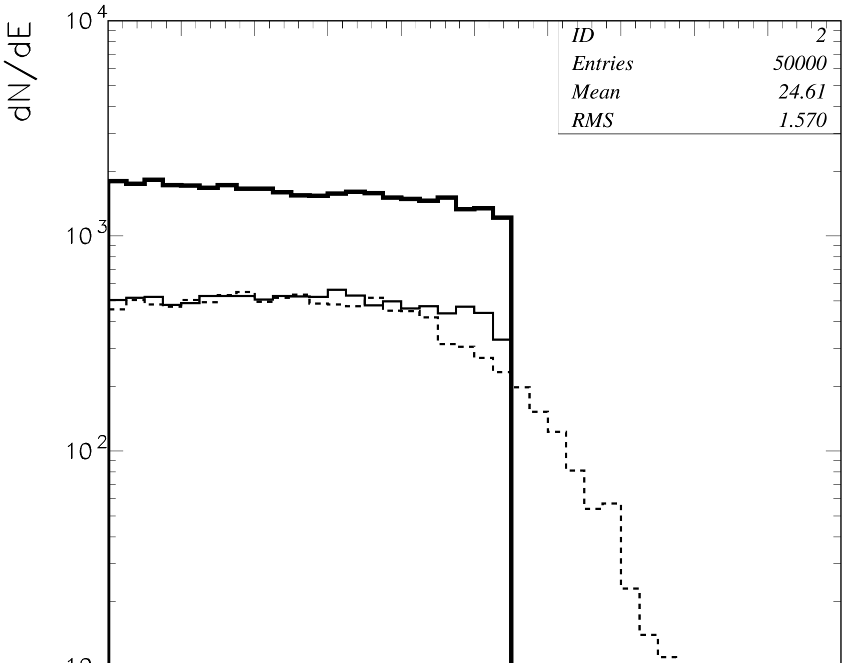

Figure 10: Photon energy spectrum distribution as measured by the lumi spectrometer. The initial photon spectrum is represented by the thick full line, the thin full line shows the spectrum of coincidences in the spectrometer acceptance without any detector resolution and the dashed line shows the measured spectrum of the coincidences in the acceptance (detector resolution folded).

In figure 11 the measured photon spectrum (dashed line) and the corresponding generated spectrum of coincidences in the spectrometer acceptance are shown in the linear scale. The actual end-point position can be obtained by fitting the mea-

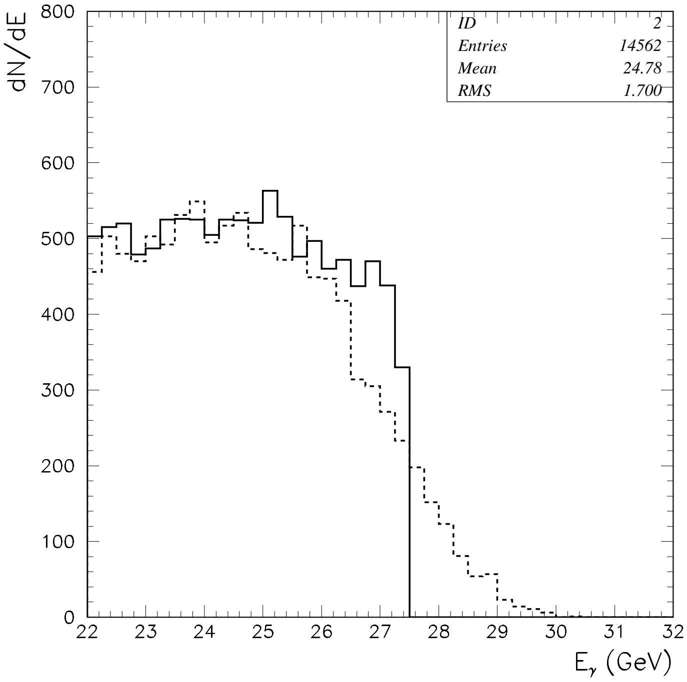

Figure 11: Photon energy spectrum distribution as measured by the lumi spectrometer. The thin full line shows the spectrum of coincidences in the spectrometer acceptance without any detector resolution and the dashed line shows the measured spectrum of coincidences in the acceptance (detector resolution folded).

sured spectrum with the theoretical acceptance function that includes the known spectrometer resolution. As the plot shows, the spectrometer measured photon distribution goes from a flat distribution from 22 to 25.5 GeV, to a rapidly falling distribution between 25.5 and 30 GeV.

4.3 Sensitivity in the BPC fiducial volume

In this section we study the sensitivity of the luminosity spectrometer in the size of the BPC fiducial volume. To estimate this sensitivity we introduce an 1mm uncertainty along the two directions that define the face of the BPCs. The effect of this fiducial surface increase in the acceptance is shown in fig. 12. In figure 13, the induced change in the overall acceptance is shown after folding in the conversion

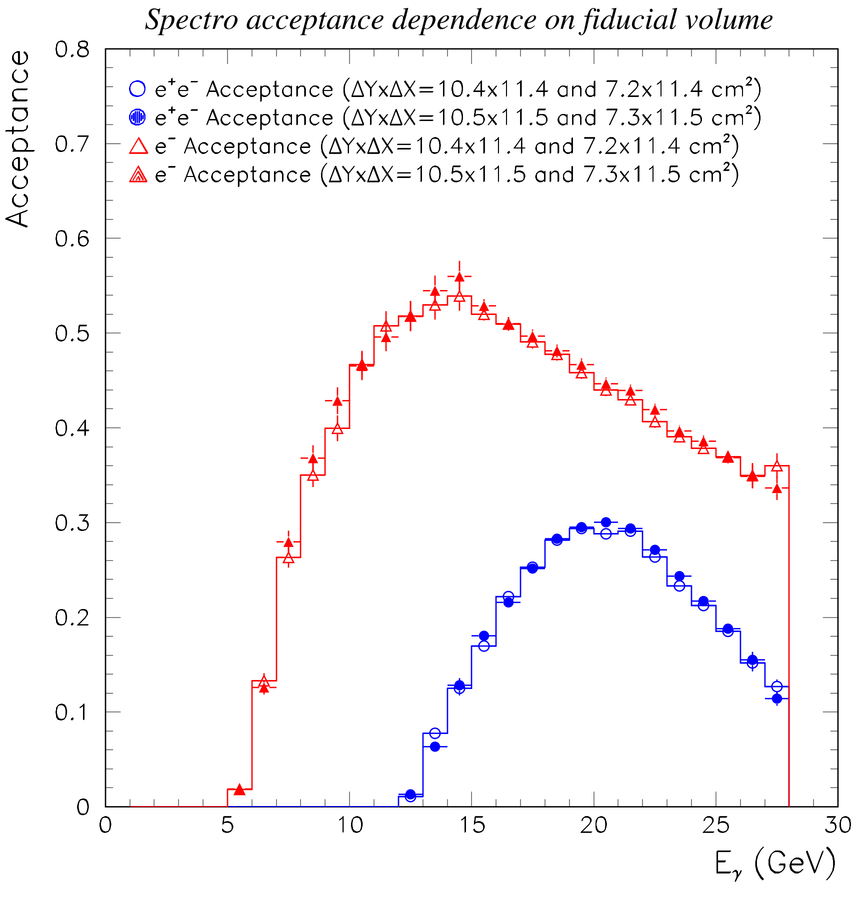

Figure 12: Acceptance dependence on the Calorimeter fiducial volume.

factor and the photon energy spectrum. As shown, the relative change is in the order of 2%. The relative change for the single electron acceptance is between 1-2%. This contributes to the pile-up systematic error. The errorbars correspond to the statistical error of the MC calculation.

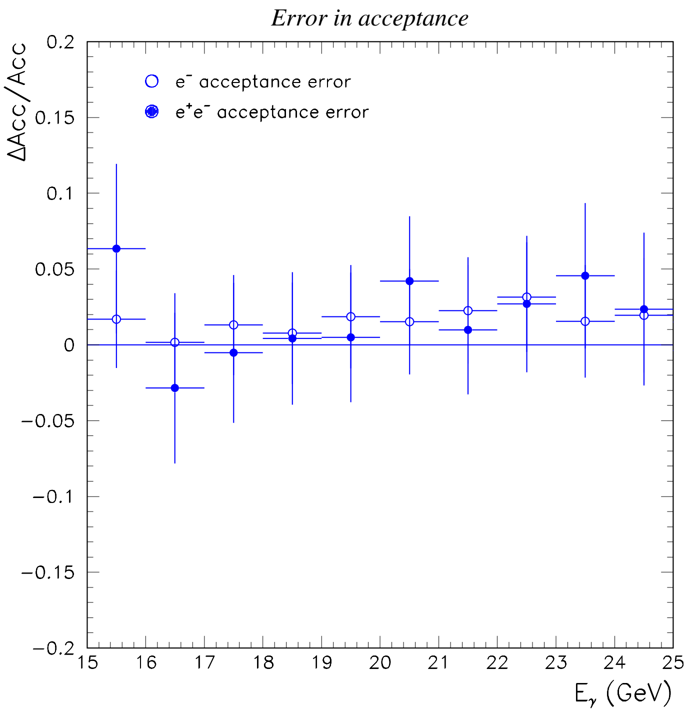

Figure 13: Acceptance relative change as a function of the photon energy.

4.4 Sensitivity in photon beam position and distribution

Here we study the sensitivity of the spectrometer in variations in the photon beam position and distribution at the exit window. In fig. 14 the photon beam mean position was shifted by 5mm along both X and Y. This shift affects significantly only the electron acceptance with consequences in the pile-up determination. The induced error in the pile-up determination will be discussed in section 5.3. The

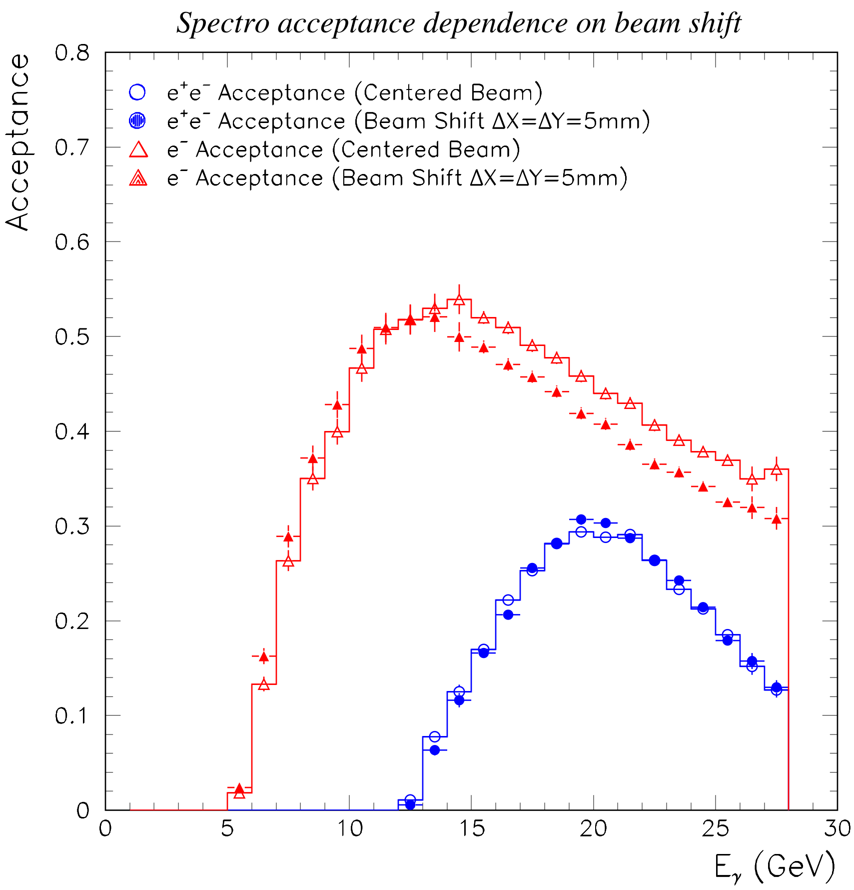

Figure 14: Acceptance dependence on photon beam position shift.

addition of an error in the spread of the photon beam by increasing the gaussian σ along X and Y, does not significantly change the results, as shown in fig. 15. In this simulation energy bins from 15 to 25 GeV have much higher statistics in order to reduce the statistical error. In figure 16, the induced change in the overall acceptance is shown after folding in the conversion factor and the photon energy spectrum. As shown, the relative change in the coincidences acceptance is in the order of 1-2%. The change for the single electron acceptance is about 8%.

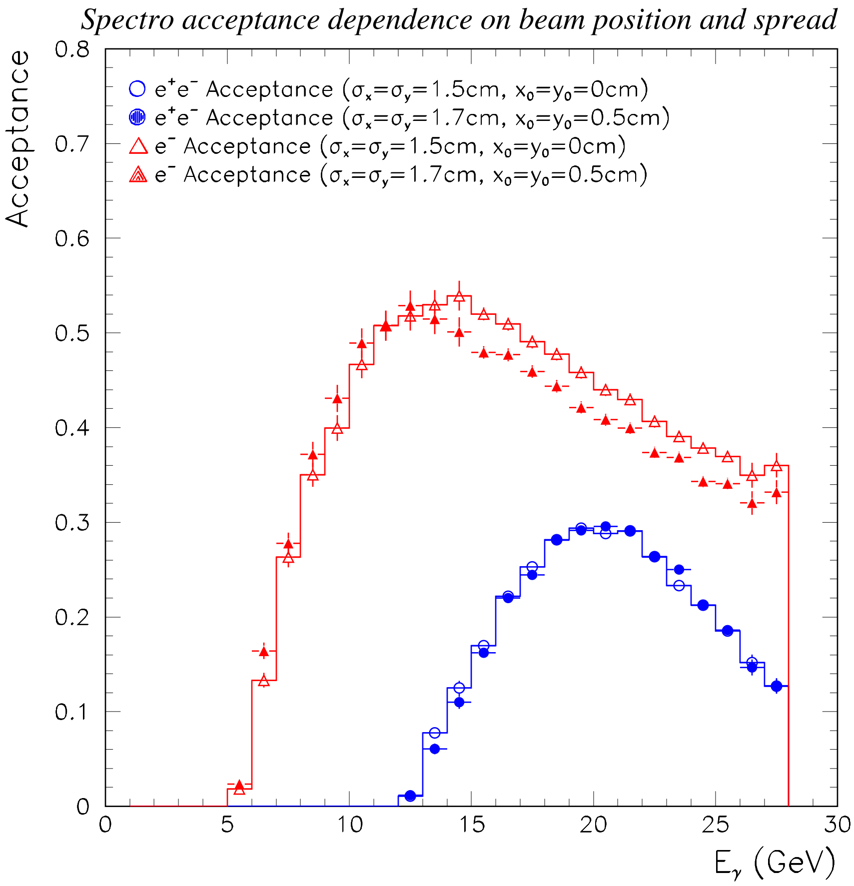

Figure 15: Acceptance dependence on photon beam spread and position.

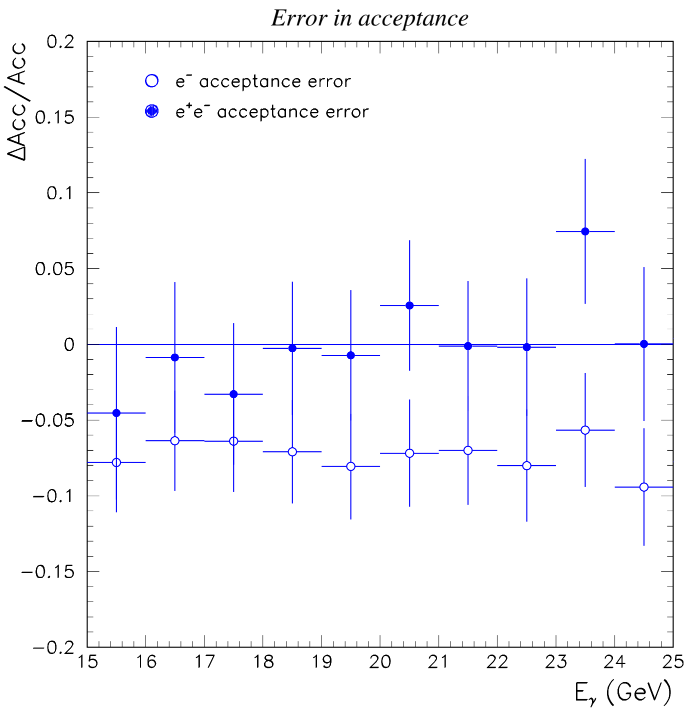

Figure 16: Acceptance relative change as a function of the photon energy for $\Delta X = \Delta Y = 5mm$, $\sigma_x = \sigma_y = 1.7cm$ versus $\Delta X = \Delta Y = 0$, $\sigma_x = \sigma_y = 1.5cm$.

4.5 Variations in the magnetic field

In this section the sensitivity of spectrometer in magnetic field variations is studied. To estimate this sensitivity, the magnetic field was varied by 2% from its nominal value and the acceptance was calculated and compared for both configurations. The result is shown in fig. 17. In figure 18, the induced change in the overall acceptance

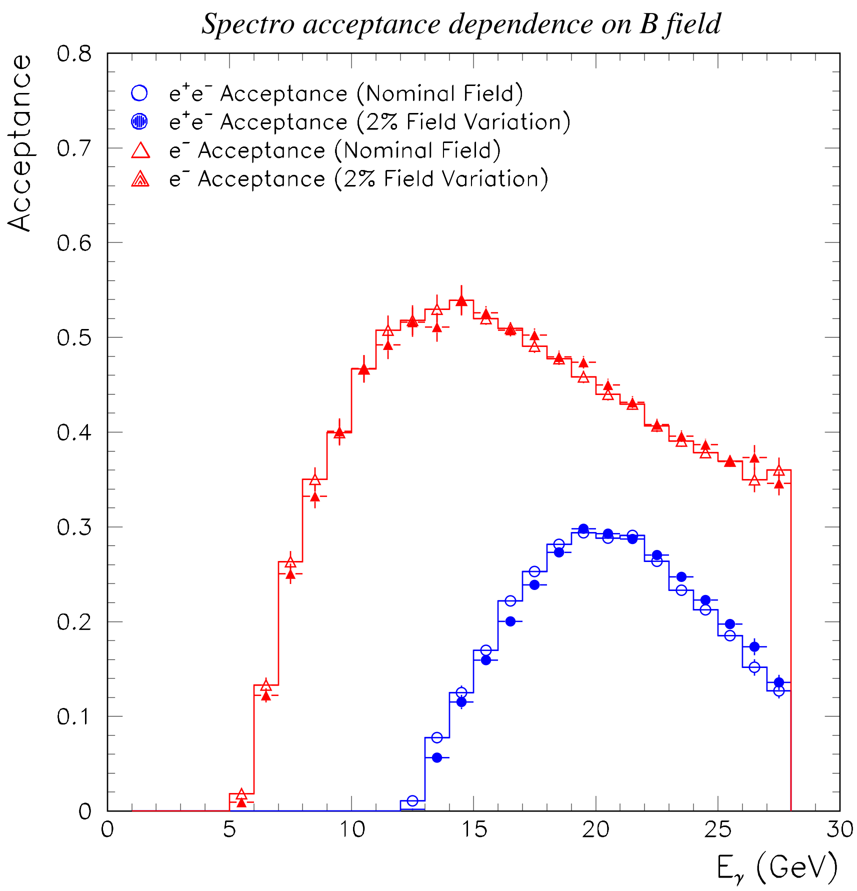

Figure 17: Acceptance dependence on magnetic field variations.

is shown after folding in the conversion factor and the photon energy spectrum. As shown, the relative change in the coincidences acceptance and the single electron acceptance is about 2% in the measuring photon energy window.

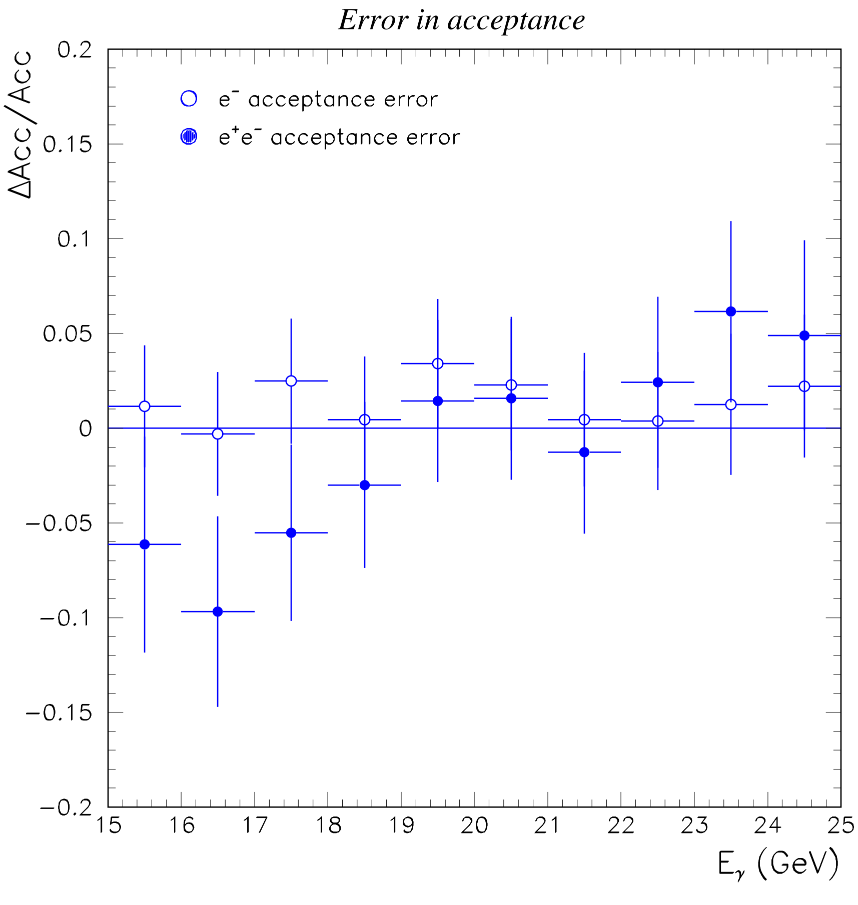

Figure 18: Acceptance relative change as a function of the photon energy for 2% variation of the magnetic field.

4.6 Spectrometer rates of single and multiple events

In this section we calculate the spectrometer rates for single and multiple (pile-up) e^+e^- events from γ conversion for two values of the specific luminosity: standard $L = 10^{31} cm^{-2} s^{-1}$, and peak $L = 7 \times 10^{31} cm^{-2} s^{-1}$. The cross-section for the process $ep \rightarrow ep\gamma$ is taken from the Bethe-Heitler formula [8]:

$$\frac{d\sigma}{dE_\gamma} = 4\alpha r_e^2 \frac{E_{e'}}{E_\gamma E_e} \left(\frac{E_e}{E_{e'}} + \frac{E_{e'}}{E_e} - \frac{2}{3}\right)\left(ln \frac{4E_p E_e E_{e'}}{M m E_\gamma} - \frac{1}{2}\right), \tag{11}$$

where $E_\gamma, E_e, E_{e'}, E_p$ are the photon, electron in, electron out, and proton energies. M and m are the proton and electron masses, α is the fine structure constant and r_e the Born electron radius. In fig. 19 the Bethe-Heitler cross-section is shown at the top plot. The photon number density per HERA bunch crossing and specific luminosity $L = 10^{31} cm^{-2} s^{-1}$ (refer to as standard) is shown at the bottom plot. The bunch crossing rate at HERA is 10 MHz.

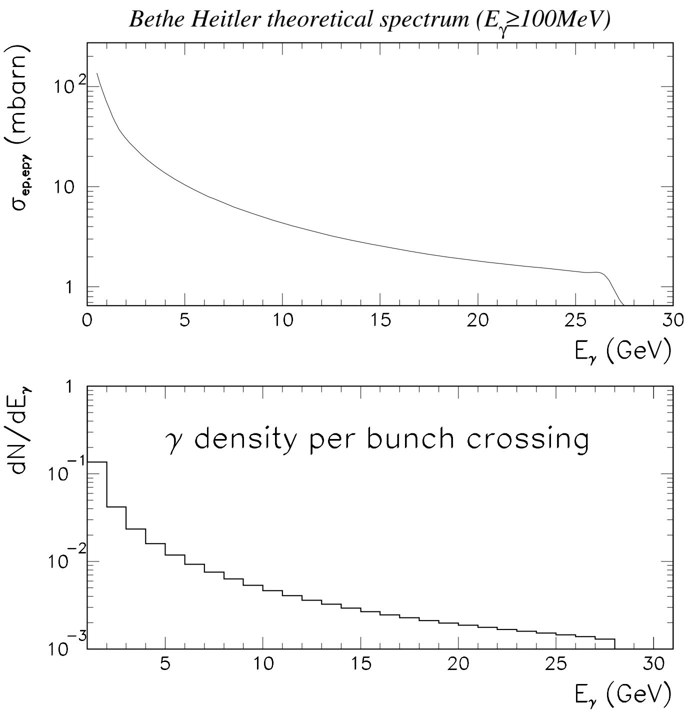

Figure 19: Cross-section (top plot) and photon density dN/dE_γ (bottom) for the process $ep \rightarrow ep\gamma$.

Using the dN/dE_γ distribution shown in fig. 19 we may obtain the single electron and e^+e^- coincidence event distribution in the BPC. The dN/dE_γ distribution for single electron events in the BPC per bunch crossing and standard luminosity is shown in fig. 20 (top plot) together with the running sum of the distribution (bottom plot). The running sum shows that for standard luminosity we should expect 3.62×10^{-3} single electron hits in the BPC per bunch crossing. This translates to a rate of 36 kHz in single electrons (standard luminosity). The dN/dE_γ distribution for

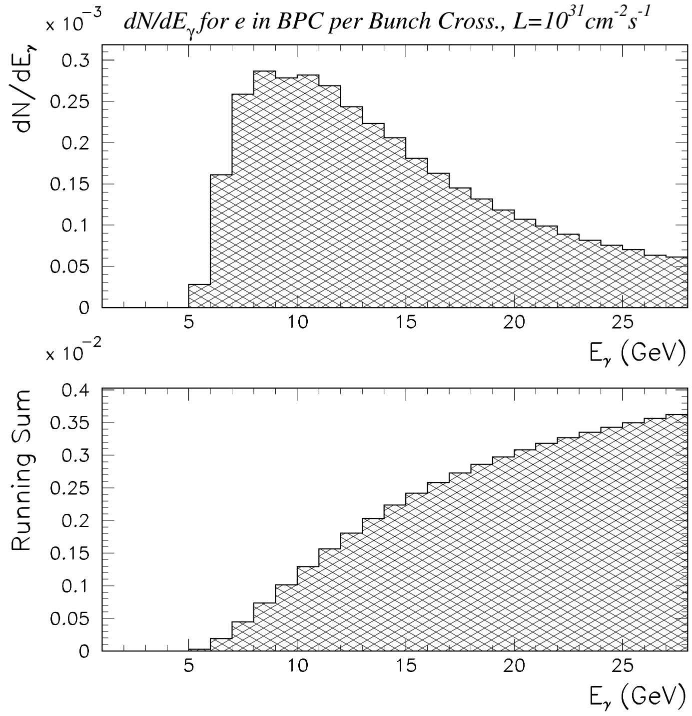

Figure 20: $\mathrm{dN/dE}_\gamma$ for single electron events in the BPC per bunch crossing and standard luminosity (top) and the corresponding running sum.

e^+e^- coincidences in the BPC per bunch crossing and standard luminosity is shown in fig. 21 (top) together with the running sum. The running sum shows that for standard luminosity we should expect 8.13×10^{-4} coincidences in the BPC per bunch crossing. This translates to a rate of 8 kHz in e^+e^- coincidences. (standard luminosity).

The rate of single electron hits in the BPC scales linearly with luminosity. High single electron rates may create a large number of fake coincidences (i.e. events where the electron and the positron come from different converted photons), and overlayed electron events (i.e. events where there is a good coincidence and an overlayed single electron hit increasing the measured photon energy). In table 1 the various BPC rates for single events, good and fake coincidences, overlayed events and signal to background ratios are shown for both the full photon energy range

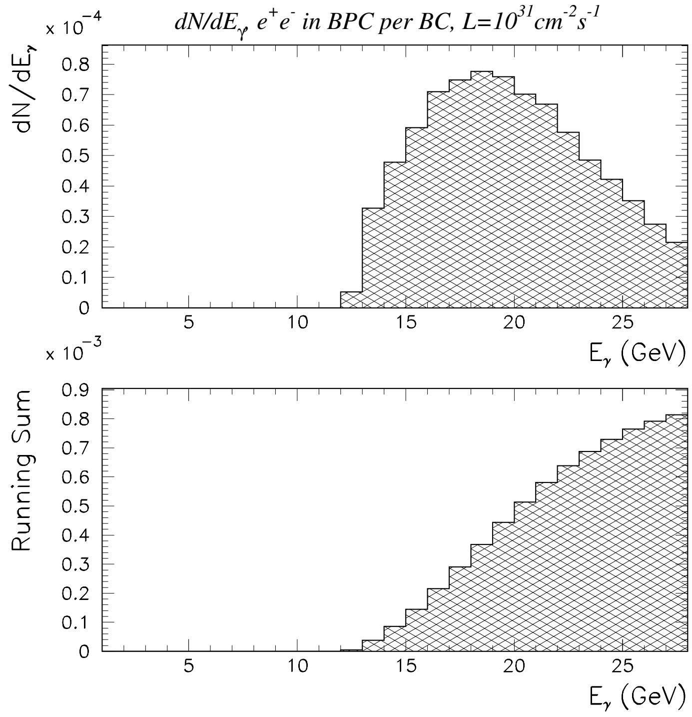

Figure 21: dN/dE$_\gamma$ for e^+e^- coincidences in the BPC per bunch crossing and standard luminosity (top) and the corresponding running sum.

and a 5 GeV window (18-23 GeV). Here is a description of the various entries in the table:

- e^- per bunch crossing: single electron rates per bunch crossing in large BPC.
- e^+ per bunch crossing: single positron rates per bunch crossing in small BPC.
- e^+e^- per bunch crossing: coincidence rates.
- Fake e^+e^- per bunch crossing: coincidences from different photons.
- Overlayed e^- per bunch crossing: events for which there is an electron hit on top of a good coincidence.
- $\mathrm{Bgnd}_{e^-}/\mathrm{Signal}_{e^+e^-}$: Ratio between rates of overlayed events and good coincidences.
- e^+e^- per bc in E_γ window: good coincidences in 5 GeV photon energy window.
- Fake e^+e^- per bc in E_γ window: coincidences from different photons in 5 GeV window.
- $\mathrm{Bgnd}_{e^+e^-}/\mathrm{Signal}_{e^+e^-}$ (window): Ratio between rates of fake coincidences and good coincidences in window.
- $\mathrm{Bgnd}_{e^+e^-}/\mathrm{Signal}_{e^+e^-}$ (z-cut): Previous ratio when a $z = E_e/E_\gamma$ cut-off has been applied.
- Rates of e^+e^- (5 GeV window): Rates (in Hz) of good coincidences in BPC.
- Probability of an overlay in window: This is the portion of the integrated number of overlays that gives a total measured photon energy in the photon 5 GeV window.
- Migrations in window per bc: This is the number of overlayed events that have a measured photon energy inside the window. It is obtained from the previous entry and it consists one of the multiple event (pile-up) background sources.
- Migrations out of window per bc: This is the number of overlayed events that have a measured photon energy outside the energy window while the actual photon energy that gave the good coincidence was inside the window. In this case the extra electron energy causes migration out of the 5 GeV window.

Description	$L = 10^{31} cm^{-2} s^{-1}$	$L = 7.10^{31} cm^{-2} s^{-1}$
e^- per bunch crossing (large BPC)	3.62×10^{-3}	$\times 7$
e^- per bunch crossing (small BPC)	2.65×10^{-3}	$\times 7$
e^+e^- per bunch crossing	8.13×10^{-4}	$\times 7$
Fake e^+e^- per bunch crossing	9.59×10^{-6}	$\times 49$
Overlayed e^- per bunch crossing	2.55×10^{-6}	$\times 49$
$\mathrm{Bgnd}_{e^-}/\mathrm{Signal}_{e^+e^-}$	0.31%	2.17%
Description (5 GeV window)	$L = 10^{31} cm^{-2} s^{-1}$	$L = 7.10^{31} cm^{-2} s^{-1}$
e^+e^- per bc in E_γ window	3.12×10^{-4}	$\times 7$
Fake e^+e^- per bc in E_γ window	2.68×10^{-6}	$\times 49$
$\mathrm{Bgnd}_{e^+e^-}/\mathrm{Signal}_{e^+e^-}$ (window)	0.86%	6.02%
$\mathrm{Bgnd}_{e^+e^-}/\mathrm{Signal}_{e^+e^-}$ (z-cut)	0.67%	4.73%
Rates of e^+e^- (5 GeV window)	3.12 kHz	21.84 kHz
Probability of an overlay in window	10.07%	
Migrations in window per bc	2.72×10^{-7}	$\times 49$
$\mathrm{Bgnd}_{IN}/\mathrm{Signal}_{e^+e^-}$ (window)	0.087%	0.61%
Migrations out of window per bc	2.55×10^{-6}	$\times 49$
$\mathrm{Bgnd}_{OUT}/\mathrm{Signal}_{e^+e^-}$ (window)	0.81%	5.72%

Table 1: Luminosity spectrometer rates.

4.7 Photon beam profile determination

Knowledge of the photon beam profile at the exit window is of great importance because it allows beam condition monitoring. The luminosity spectrometer capabilities in determining the photon profile are presented in this section. The important quantities estimated in this section are listed below:

- The accuracy in finding the vertex of the conversion.
- The accuracy in determining the width of the photon distribution in both dimensions.
- The accuracy in finding the mean.
- The statistics needed in order to observe shifts in the beam spot and the sensitivity in the magnitude of these shifts.

4.7.1 Method

The method used to extract the e^+e^- origin is described here. In fig. 22 a schematic view is shown. The e^+e^- origin Y coordinate Y_{hit} is approximated as the energy-weighted position of the two electrons as measured in the BPC's:

$$Y_{hit} = \frac{E^+ \cdot BPC^+ + Y^- \cdot BPC^-}{E^+ + E^-} \tag{12}$$

where E^+, BPC^+ and E^-, BPC^- the energies and positions of the e^+ and e^- as obtained from the BPC's.

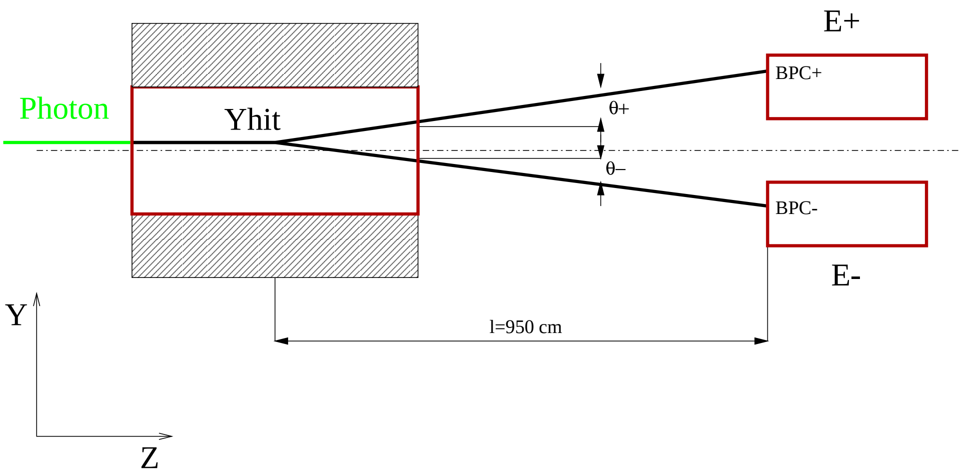

Figure 22: Method for obtaining the photon profile.

4.7.2 Resolution in Y

In this section we calculate the resolution in the Y coordinate of the photon conversion as obtained from the method outlined in the previous section. This resolution depends on the BPC position and energy resolution.

The BPC position resolution depends on the incident electron energy. This dependence is described in fig. 23 from [9]. From this figure one can see that the

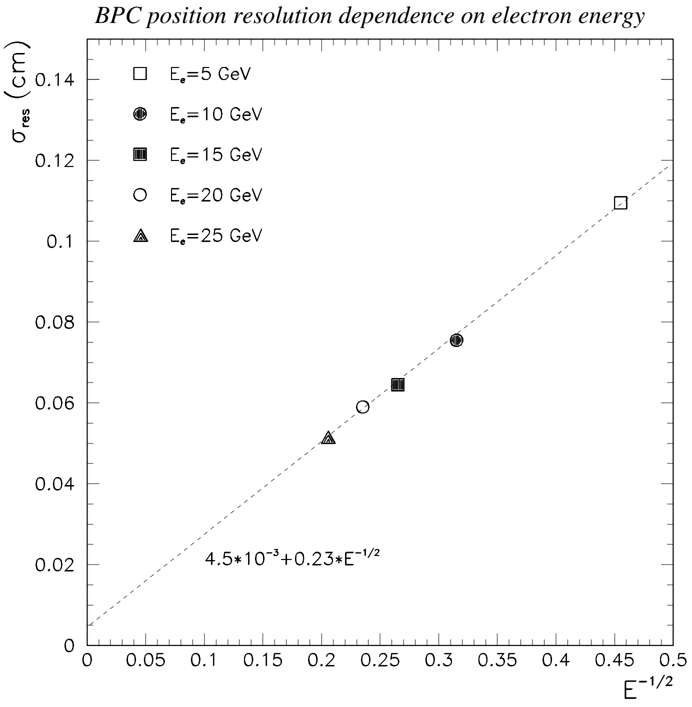

Figure 23: BPC position resolution dependence on electron energy. The energy relevant to the luminocity spectrometer is centered at 10 GeV where the BPC position resolution is 0.7 mm.

BPC resolution for a 10 GeV electron is around 0.7 mm. The BPC energy resolution is also energy dependent and is typically parametrized as:

$$\frac{\sigma_E}{E} = \frac{a}{\sqrt{E_e}} \oplus b \tag{13}$$

where a and b are parameters (for a discussion see section 5.1).

Based on the known BPC position and energy resolution, the Y_{hit} distribution of the photon profile was reconstructed (fig. 24). In this simulation a beam of 100000 photons hit the exit window with a gaussian distribution in both x and y with mean at $x = y = 0$ and $\sigma_x = \sigma_y = 1.5cm$. The resolution obtained is around 5 mm.

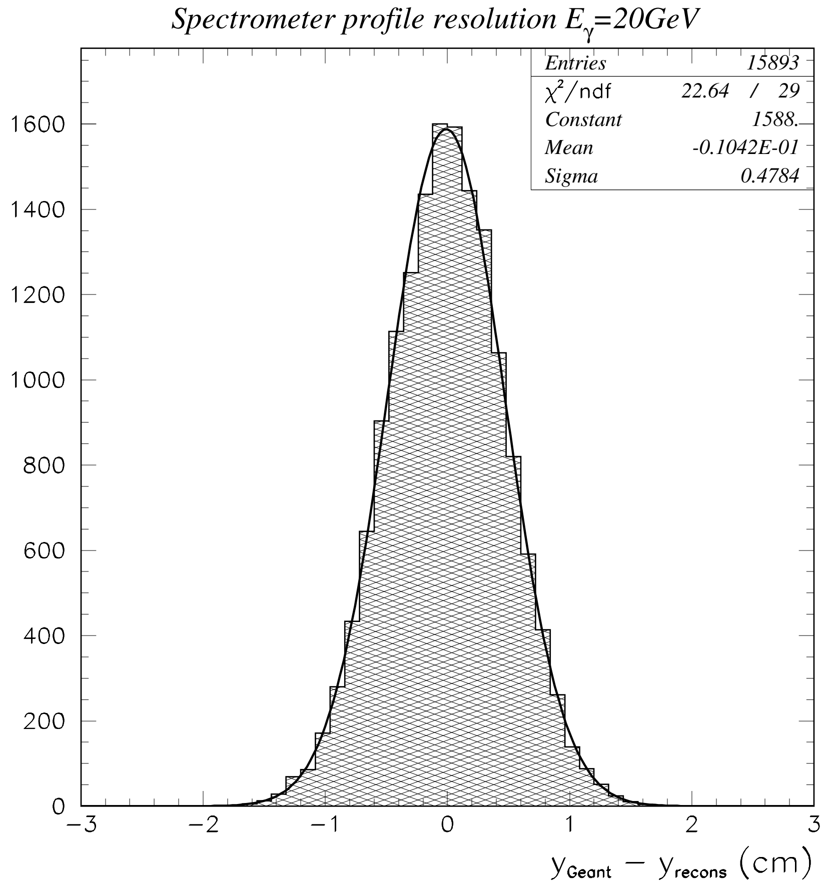

Figure 24: Luminosity spectrometer photon conversion position resolution (y-coordinate in cm).

From the same analysis the photon profile obtained is shown in fig. 25. The reconstructed y coordinate of the photon profile (top) is compared to the Geant profile for all accepted coincidences. It should be stressed that the bottom plot (i.e. Geant plot) contains only the photons that gave coincidences in the BPC. This is the reason why the σ of the fit is not exactly 1.5 cm as it would if all conversions were plotted. On the other hand, the top plot is in good agreement in both the

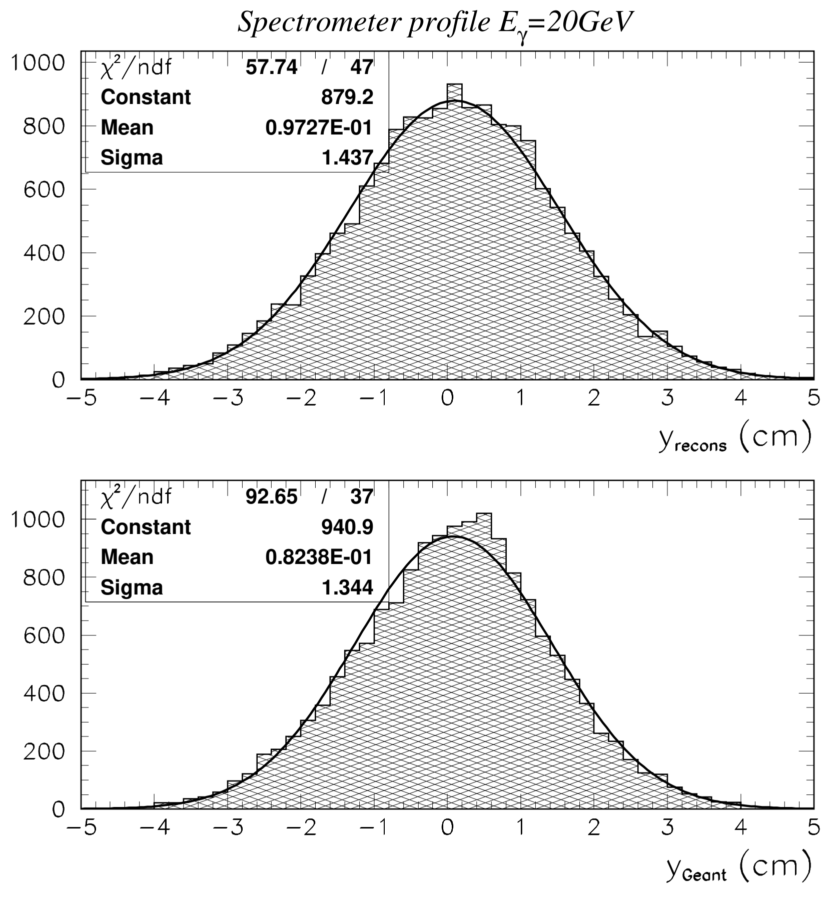

Figure 25: Photon profile determination using the luminosity spectrometer. The reconstructed y coordinate of the photon profile (top) is compared to the Geant profile for all accepted coincidences.

mean and the σ with the Geant plot.

4.7.3 Sensitivity in photon beam spot shifts

The analysis done in the previous section does not answer the question on the spectrometer sensitivity in beam shifts. To estimate this sensitivity we sent 100000 photons with total momentum of 20 GeV to hit the beam pipe window with a gaussian distribution in both x and y with mean at $x = y = 8mm$ and $\sigma_x = \sigma_y = 1.5cm$. Now the beam is shifted by 8mm in x and 8mm in y. The reconstructed Y distribution is shown in fig. 26. Again we observe that the reconstructed profile follows the shift in the mean of the actual profile. Again one should notice that the actual profile seen is not at 8mm as it should because of the spectrometer acceptance. The reconstructed profile for a $\Delta X = \Delta Y = 2mm$ shift is shown if fig. 27. In this

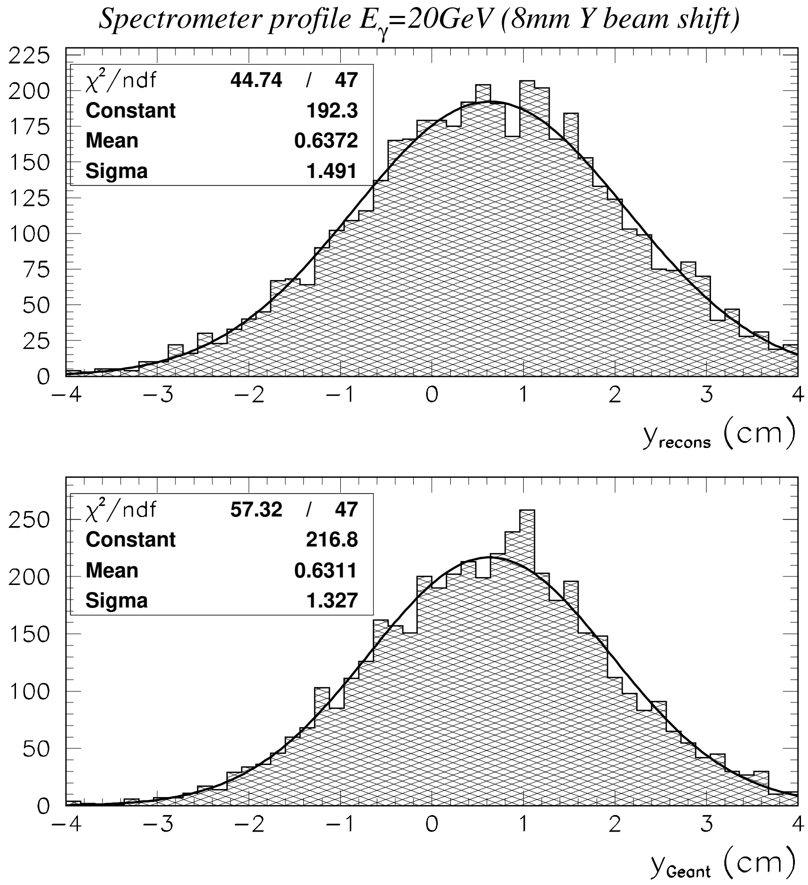

Figure 26: Beam profile reconstruction for a beam shifted in X and Y by 8mm.

case the reconstructed mean is $\simeq 1.7mm$. The spectrometer is still sensitive in the beam shift.

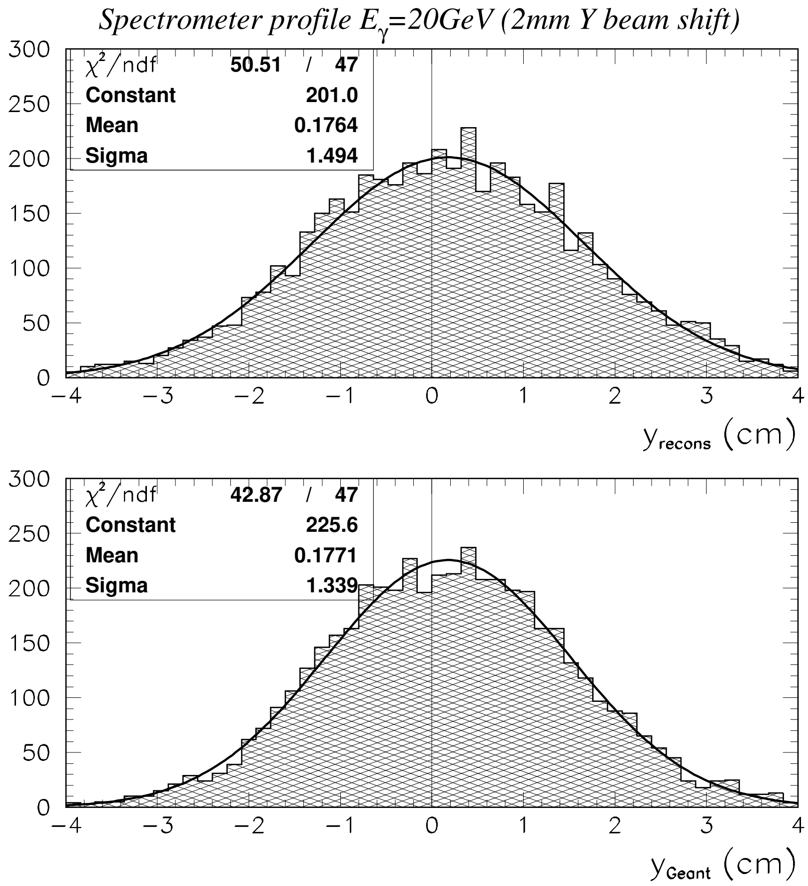

Figure 27: Beam profile reconstruction for a beam shifted in X and Y by 2mm.

Our conclusion from these studies is that the spectrometer sensitivity in photon beam shifts is better than 1-2 mm. This is a good result since it allows for a reliable monitoring of the beam. The number of events needed in order to observe such change is 5000-10000 events. As we have seen the spectrometer rates are 3 kHz for standard luminosity and 20 kHz for peak luminosity. This means that the photon beam can be monitored every second or so with a sensitivity in shifts better than 2 mm.

Test	a	b	Boundary Shift	σ^{BH} (mb)	Total Error
Test 1	0.	0.	0.%	8.908826	0.
Test 2	0.2	0.01	0.%	8.908762	0.001%
Test 3	0.2	0.01	0.5%	8.865372	0.4878%
Test 4	0.2	0.02	0.5%	8.865236	0.4893%
Test 5	0.17	0.02	0.5%	8.865623	0.4850%
Test 6	0.2	0.02	1%	8.822408	0.97%

Table 2: Errors in the cross section calculation.
endcenter

5 Systematic Errors

5.1 Energy Scale and resolution uncertainties in the cross section determination

BPC energy scale errors induce an error in the calculation of the Bremsstrahlung cross-section within an energy window. To calculate this error we parametrize the BPC resolution as follows:

$$\frac{\sigma_E}{E} = \frac{a}{\sqrt{E_{e^\pm}}} \oplus b \tag{14}$$

The total bremsstrahlung cross section is:

$$\sigma^{BH} = \int_{E_1}^{E_2} \frac{d\sigma^{BH}}{dE_\gamma} \otimes g(E_\gamma) dE_\gamma \tag{15}$$

The convolution with the detector response $g(E_\gamma)$ gives in detail:

$$\sigma^{BH} = \int_{E_1}^{E_2} [\int \frac{d\sigma^{BH}}{dE'_\gamma} \frac{1}{\sqrt{2\pi}\sigma} e^{-(E'_\gamma - E_\gamma)^2/2\sigma^2} dE'_\gamma] dE_\gamma \tag{16}$$

To estimate the error in the calculation of the cross-section based on equation 16, we performed the integral varying parameters a, b and the systematic shift of the energy window boundaries E_1 and E_2. The range that parameters a and b can vary is known [9], while a reasonable value for the boundary shift is 0.5%. From the results shown in table 2, we conclude that with realistic detector response parameters (tests 3,4,5) we get an error less than $\simeq 0.5\%$. If we examine the extreme case where the window boundaries are shifted by 1% the total error is slightly below 1%.

5.2 Theoretical cross-section error

The calculation presented in the previous section did not include errors in the knowledge of the theoretical cross-section Bethe-Heitler formula.

It was estimated before the ZEUS luminosity upgrade that this error was $\simeq 0.4 - 1.2\%$ depending on the bremsstrahlung photon energy [6], [7]. It is one of the advantages of the technique studied in this report that the spectrometer measures the luminosity at an energy range ($18 - 23 GeV$) for which the theoretical calculation gives a minimum error ($< 0.5\%$). In this note we will assume that $\delta\sigma_{BH}/\sigma_{BH} < 0.5\%$ at peak luminosity.

5.3 Multiple events correction errors (pile-up)

As we have seen in section 4.6 there is a significant probability for multiple events to occur especially for peak luminosity ($7 \times 10^{31} cm^{-2} s^{-1}$) (table 1). These pile-up events create background coincidences, migration of good coincidences out of the BPC acceptance window, and migrations of lower energy coincidences in the window. As a result the rates measured have to be corrected for these effects. The correction factor $f(R_2)$ is rate dependent and is obtained from calculation.

The calculation of the systematic error here assumes no knowledge of the single electron acceptance as in the case of the good coincidences (using the 6 meter tagger). In fact, there are techniques which can provide information on the singles acceptance. Examples are events with two hits in the same BPC and coincidence events where the total photon energy is above the end-point. Such techniques are under investigation and are expected to reduce the pile-up systematic error calculated in this section.

Uncertainties in the BPC fiducial volume, in the beam position and distribution and energy scale errors, contribute to the pile-up induced systematic error. As is shown below, although the error in the single electron acceptance from these effects is in the order of 5-10%, the correction itself is less than 10% (at peak luminosity) thus inducing a $< 1\%$ systematic error.

5.3.1 Uncertainty in the BPC fiducial volume

Uncertainties in the BPC fiducial volume induce an uncertainty in the number of background coincidences and migrations inside the rate measuring energy window and migrations out of the window. Background coincidences occur when an electron and a positron from two different photons leave hits in the spectrometer. As we have seen in figures 12 and 13, the photon energy distributions which give electron hits in the BPC do not vary significantly with the fiducial volume. The relevant quantity for background coincidences is the electron energy distribution. In figure 28 the electron energy distribution is shown for two BPC fiducial volume configurations. These electrons were produced as follows:

- 500,000 bremsstrahlung γs following the Bethe-Heitler distribution with energies $4 - 27.5$ GeV were produced.
- The photons hit the beam pipe exit window at a position that follows the gaussian distribution along x and y, with mean at $x = 0$ and $y = 0$ and $\sigma_x = \sigma_y = 1.5$ cm.

- The photons convert in the window (Geant was used to simulate the conversion).
- The conversion products were propagated as usual through the simulated magnetic field to finally hit the BPC.

Only electrons that left hits in the BPC are plotted. From these distributions we

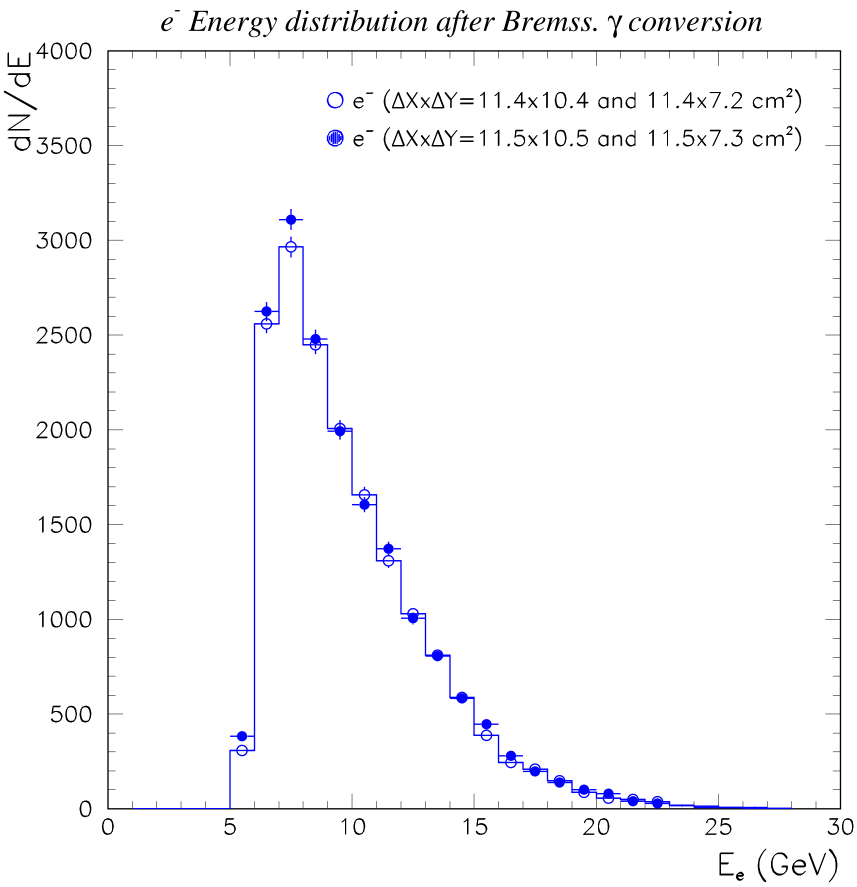

Figure 28: Electron energy dependence on the BPC fiducial volume. These electrons come from bremsstrahlung γ conversion.

calculate the variation in the background coincidences which is 0.1%. So, as expected the induced systematic error due to background coincidences is relatively small. The error in the number of migrations in and out of the energy window can be taken from figure 13. Namely, there is a $\leq 2\%$ uncertainty.

In table 3 we summarize the systematic errors due to errors in the fiducial volume of the BPC. The only non-negligible contribution to the total systematic error is for the migrations outside the spectrometer acceptance window correction. This correction is still small ($\simeq 0.1\%$).

Pile-up correction	estimated error	syst. err. $L = 10^{31}$	syst. err. $L = 7 \times 10^{31}$
Fake Coincidences	0.1%	small	small
Migrations in	2%	small	small
Migrations out	2%	small	0.11%

Table 3: Uncertainties in multiple event corrections due to uncertainties in the BPC fiducial volume. Only the peak luminosity *migrations out* systematic error is not negligible.

5.3.2 Uncertainty in photon beam position and distribution

As we saw in section 4.4 and figures 15 and 16, photon distribution variations and shifts are expected to give the biggest contributions to the pile-up systematic error. Since the electron acceptance changes by roughly 8%, we expect a similar induced error in the pile-up determination.

In figure 29 the electron energy distributions are plotted for two photon beam conditions: the expected one were the beam is centered and its spread is gaussian in both x and y with $\sigma_x = \sigma_y = 1.5\ cm$, and an extreme one where the beam is not centered and its spread has been significantly increased. From these distributions

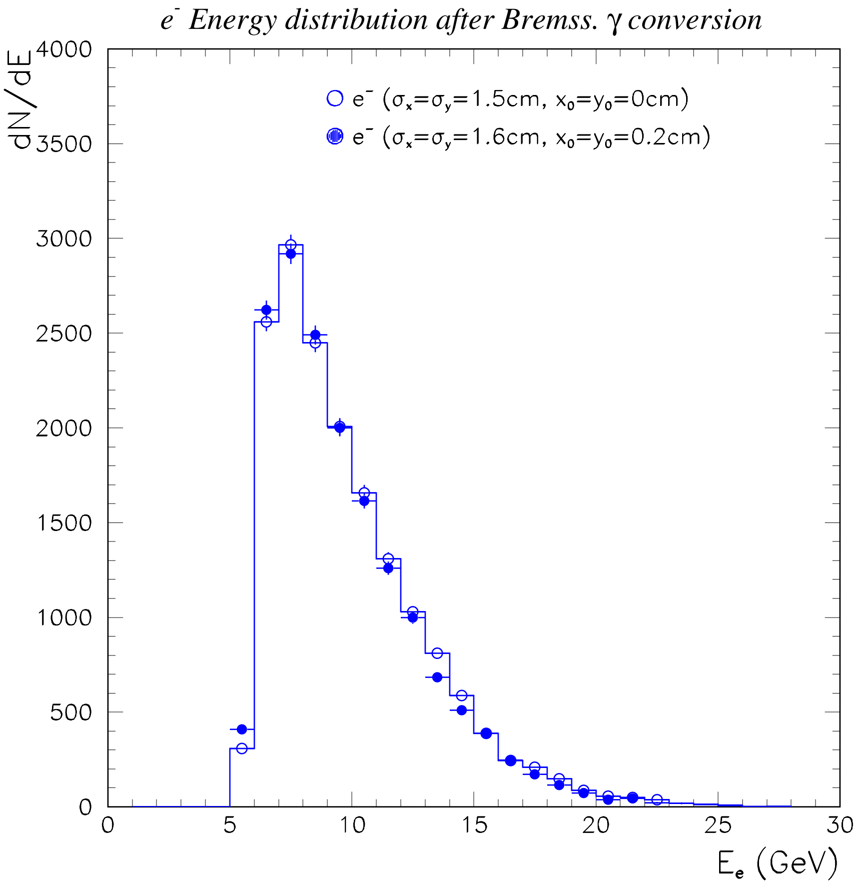

Figure 29: Electron energy dependence on beam distribution. These electrons come from bremsstrahlung γ conversion.

we calculate the variation in the background coincidences which is 4.1%. The error in the number of migrations in and out of the energy window is obtained from the calculation uncertainty of the number of single electron (or positron) hits, which is a $\leq 7\%$ uncertainty.

In table 4 we summarize the systematic errors due to a 2mm uncertainty in the mean and 1mm uncertainty in the σ of the X and Y photon profile Gaussian distributions. These errors are multiplied by the pile-up background to signal ratios (table 1) to give the corresponding systematic errors.

Pile-up correction	estimated error	syst. err. $L = 10^{31}$	syst. err. $L = 7 \times 10^{31}$
Fake Coincidences	4.1%	0.028%	0.2%
Migrations in	7%	small	0.04%
Migrations out	7%	0.057%	0.4%

Table 4: Uncertainties in multiple event corrections due to variations in the beam position and distribution ($\Delta X = \Delta Y = 2mm$, $\Delta\sigma_x = \Delta\sigma_y = 1mm$).

5.3.3 Error in the photon energy window

Uncertainties in the photon energy window contribute small errors in the total pile-up systematic error, thus we will not discuss them here.

5.4 Acceptance correction errors

As it was discussed in the introduction, the spectrometer acceptance is calculated with the help of the 6 meter electron tagging calorimeter which has close to 100% acceptance in a narrow energy window. As we will see this method keeps systematic errors in acceptance below 1% as long as the acceptance is measured simultaneously with the luminosity. In this case the acceptance is calculated from the ratio of the number of coincidences to the number of tags (see eq. 5). The corrected number of coincidences is obtained from the measured coincidences by correcting for pile-up and *egas* events. This correction is small (a few percent) and is the same one used for the luminosity measurement correction (see eq. 3 and 8). The calculated mean acceptance $\overline{a}$ also involves uncertainties due to the 6 meter tagger resolution, calculated at section 5.4.5. If the 6m tagger were not used, the calculated acceptance would have to be obtained by:

$$\overline{a} = \frac{\int_{E_1}^{E_2} a(E_\gamma) \frac{dN}{dE_\gamma} dE_\gamma}{\int_{E_1}^{E_2} \frac{dN}{dE_\gamma} dE_\gamma} \tag{17}$$

and would involve all uncertainties studied in the performance section 4 which contribute a systematic error of 5-10%! This potential disadvantage of the proposed technique is eliminated with the use of the 6m tagger. The total systematic error in the acceptance calculation obtained in this section is $< 1\%$.

5.4.1 BPC energy scale uncertainties

The spectrometer acceptance is fairly flat within a relatively large photon energy window, as it was shown in fig. 5. This means that the error induced from BPC energy scale uncertainties can be obtained from Table 2 in section 5.1. This error is expected to be in the order of 0.5% for a 0.5% shift of the window energy boundaries and nominal BPC resolution parameters.

The photon spectrum end-point $E = 27.5\ GeV$ will be used for the BPC energy calibration. This can be done over the whole BPC fiducial volume by varying the dipole magnetic field during calibration runs.

5.4.2 Off momentum beam electrons correction error

Off momentum beam electrons may generate a background in the interesting energy window of the tagger either by hitting directly the tagger or by generating electron debris after hitting nearby collimators. These background electrons have to be subtracted from the electrons registered by the 6m tagger:

$$N_{tags}^{CORRECTED} = N_{tags}^{MEAS} - N_{tags}^{OFFMOM} - N_{tags}^{EGAS}. \tag{18}$$

This correction is measured in a way similar to the *egas* background correction. The electron background in the tagger acceptance is measured using pilot bunches. This background is scaled to the bremsstrahlung e^- acceptance using the current ratio, and it is subtracted from the measured rate.

Current simulations (which are still on going) using the EGS4 code system [10], have shown that the background electron rates in the tagger acceptance are less than 5% of the signal [11]. The electron current uncertainty in peak luminosity is expected to be around 10%. This means that the total systematic error in the tagger background electron rates is less than 0.5%.

5.4.3 Multiple events correction uncertainties

The number of coincidences $N_{coinc}^{CORRECTED}$ measured by the spectrometer has to be corrected for pile-up and *egas* events during the measurement of the acceptance:

$$N_{coinc}^{CORRECTED} = N_{coinc}^{MEAS} - N_{coinc}^{PILEUP} - N_{coinc}^{EGAS} \tag{19}$$

The pile-up corrections are obtained from calculation and as we have seen (table 1), the corrections are $< 1\%$ for standard luminosity, and $< 7\%$ for peak luminosity. The error in the calculation has been estimated in section 5.3. The overall error at peak luminosity is $< 0.5\%$ and is obtained by adding in quadrature the errors in the fake coincidence, migration in and migration out corrections.

5.4.4 egas background correction error

The *egas* background correction method has been described in detail in [2], [5], [6] and more recently in [7]. As we have already presented, the correction is:

$$R_1 = R_0 - \frac{I_e^{tot}}{I_e^{pilot}} R^{pilot} \tag{20}$$

where I_e^{tot} is the total electron current, and I_e^{pilot} the electron current of the pilot bunches. Currently [7] this correction is obtained from the distribution of the average $\langle R_1/R_0 \rangle$ versus the proton current. The systematic error is estimated by observing deviations in rate to current ratios for electron pilot bunches. In the past this deviation did not exceed 3% and the amount of the background was small ($\simeq 2\%$) so that the total systematic was 0.06%. Here even if we assume that the *egas* total systematic error scales linearly with Luminosity, this error remains below 0.5%.

5.4.5 6 meter tagger energy scale and resolution uncertainties

The 6 meter target energy resolution and linearity affect the accuracy with which the acceptance is calculated for the spectrometer. The reason is that the tagger tags photons within a certain energy window (typically 3 GeV wide) for which the spectrometer looks for the corresponding converted photons. Uncertainties in the boundaries of the tagger energy window induce errors in the mean acceptance $\overline{a}$ calculation:

$$\overline{a} = C\overline{a}' \tag{21}$$

$$\overline{a}' = \frac{N_{coinc}^{CORRECTED}}{N_{tags}^{CORRECTED}} \tag{22}$$

The measured acceptance $\overline{a}'$ is related to the actual acceptance $\overline{a}$ by a factor C defined as follows:

$$C = \frac{\frac{\int_{E_1}^{E_2} a(E_\gamma)\frac{dN}{dE_\gamma}dE_\gamma}{\int_{E_1}^{E_2} \frac{dN}{dE_\gamma}dE_\gamma}}{\frac{\int_{E_1^{6m}}^{E_2^{6m}} P_6(E_\gamma)a(E_\gamma)\frac{dN}{dE_\gamma}dE_\gamma}{\int_{E_1^{6m}}^{E_2^{6m}} P_6(E_\gamma)\frac{dN}{dE_\gamma}dE_\gamma}} \tag{23}$$

The fluctuations of factor C correspond to the uncerainties in the calculation of the acceptance due to uncertainties in the tagger response (function $P_6(E_\gamma)$). These uncertainties take a minimum value in the case shown in figure 30. In this figure, the tagger electron energy window boundaries are systematically shifted within an energy range for which the spectrometer photon acceptance is flat. When the photon energy distribution measured by the spectrometer is flat within an energy window of 5 GeV, the tagger energy resolution has a minimum impact on the acceptance measurement.

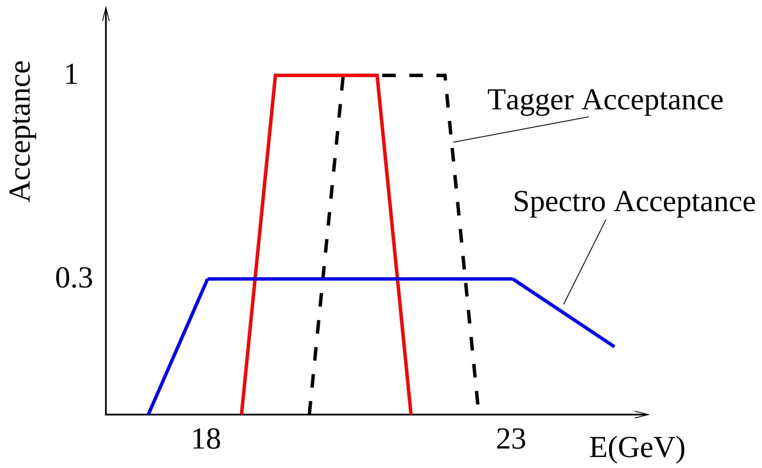

Figure 30: Tagger energy resolution and spectrometer acceptance uncertainty.

Test	a^{6m}	b^{6m}	Boundary Shift	Factor C	Total Error in Acceptance
Test 1	0.	0.	0. %	1.0	0.
Test 2	0.2	0.01	0.0%	0.999994	6×10^{-6}
Test 3	0.	0.	0.5%	1.005173	0.517%
Test 4	0.2	0.01	0.5%	1.005194	0.519%

Table 5: Uncertainty in the acceptance calculation due to the 6m tagger resolution.

In this section we calculate the uncertainty in the determination of factor C. The spectrometer acceptance shown in figure 5 is assumed while the tagger resolution is varied. The tagger resolution is given by:

$$\frac{\sigma_E}{E} = \frac{a^{6m}}{\sqrt{E_e}} \oplus b^{6m} \tag{24}$$

In table 5 the uncertainty in the acceptance is shown. The acceptance error depends directly on the knowledge of the 6m tagger energy scale. In the study we shift the spectrometer boundary energies by 0.5% (maximum). The spectrometer acceptance window is centered (roughly) at 21 GeV. This corresponds to $\simeq 100 MeV$. The tagger corresponding energy is about 7 GeV so this is 100MeV/7GeV required escale for the tagger. We expect to calibrate the tagger using the spectrometer and the relation $E_\gamma + E_e = 27.5 GeV$. Hence the required scale error for the 6 m tagger is about 3 times that of the spectrometer, or about 1.5%. As shown the expected uncertainty in the acceptance calculation due to the 6m tagger resolution is 0.52%.

In summary, the total systematic error due to the acceptance calculation is about 1% or less.

5.5 Summary of the systematic errors

A summary of the systematic errors is given in table 6. The counting, thermal γ

Error Type	$L = 10^{31} cm^{-2}s^{-1}$	$L = 7.10^{31}$
Multiple event correction		$\leq 0.5\%$
egas bgnd subtraction		$\leq 0.5\%$
Total Acceptance error		$\leq 1.0\%$
Energy Scale errors	-	$\leq 0.5\%$
Cross-section Calculation	-	$\leq 0.5\%$
Total systematic error		$\leq 1.4\%$

Table 6: Systematic Error in luminosity measurement of proposed Lumi Spectrometer for two values of HERA specific luminosity.

background and p-beam background errors are currently expected to be relatively low so they are not taken into account. The theoretical calculation of the cross section error was taken as 0.5%. The total systematic error is calculated by summing all errors in quadrature. The total systematic error is expected to be below 1.4%.

6 Beam Pipe Calorimeter

In this section we review the hardware requirements for the luminosity spectrometer and we list the Beam Pipe Calorimeter characteristics.

6.1 BPC characteristics

The BPC consists of two segmented tungsten-scintillator sampling calorimeter modules. Each of the modules consists of 26 3.5 mm tungsten alloy plates and 26 2.6 mm thick scintillator finger. Each scintillator finger is 7.9 mm wide. On the top and bottom there are two 5mm tungsten bars. The layout is shown in fig. 31. The scintillator planes have a matrix arrangement for X and Y position reconstruction. Vertically oriented fingers provide X reconstruction (X planes). One of the modules has 11 fingers per X plane (88 mm total active length along X), while the other has 15 fingers per X plane (120 mm active length). Horizontally oriented fingers provide Y reconstruction (Y planes). Both modules have 16 fingers per Y plane (128 mm active length along Y). The overall length of the passive layers corresponds to $24X_0$ (radiation lengths) which is sufficient for longitudinal shower containment for electrons up to 27.5 GeV.

Some of the BPC characteristics are listed in table 7. These characteristics together with actual BPC module sizes were used in all simulations used in this study.

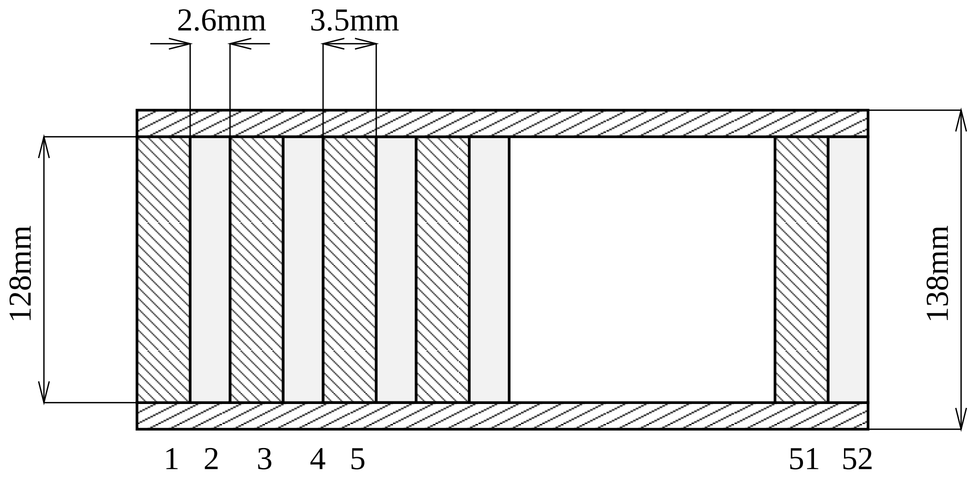

Figure 31: YZ view of the BPC module layout.

BPC specification	BPC performance
Depth	$24X_0$
Moliere radius	$13mm$
Energy resolution	$17\%/\sqrt{E}$ (stochastic term)
Energy scale calibration	$\pm 0.5\%$
Energy uniformity	$\pm 0.5\%$
Linearity	$\leq 1\%$
Position resolution	$< 1mm$
Time resolution	$< 1ns$

Table 7: BPC performance specifications

7 Costs, Manpower and Timetable

The estimated costs of the luminosity spectrometer are shown in table 8. One item that has not been clarified yet is if a compensating magnet will be used. HERA physicists are performing studies to see if an appropriate shielding would suffice. It was estimated that 10 spare Hamamatsu miniature photomultipliers (R7400) need to be purchased. Certain modifications have to be performed in the current BPC. The most important is the reconstruction of the scintillator fingers read out for the smaller (BPC south) module. Namely, the X finger wavelength shifting bars (WLS) which are currently bent by 90° overlap with the proton beam pipe. One solution to this problem is to use straight WLS bars and read the X fingers from the back of the small BPC module. A new vacuum pipe has to be built and placed between the exit

Overall Cost Estimate	
item	*price (kDM)*
Dipole Magnet	50
Compensating Magnet (?)	50
Cone-shape vacuum beam pipe	20
Magnet mechanical support	4
BPC mechanical support	4
Spare PMTs (R7400)	10
BPC modifications	2
Contingency	40
total	180(estim)

Table 8: Cost estimate table.

Manpower				
Institutes	Money (kDM)	People		Tasks
		Phys.	Eng.	
Columbia	50	2.5		Coordination, beam tests, software online-offline analysis
DESY	50	1	1	Magnet, assembly, mechanics, Beam Pipe
Yale	TBD	1	1	Electronics
TBD				BPC Modifications, electronics

Table 9: Institutes Involved.

window and the two BPC modules. The vacuum pipe will have a cone shape after the bending magnet. A new electronics read-out design will be used in order to handle the higher rates. This design was originally proposed for the HERA polarimeter by the Yale group and meets the requirements of the spectrometer read-out.

The various institutes involved in the spectrometer project are listed in table 9. The timetable of the project depends on the HERA year 2000 shutdown schedule. The read-out electronics construction will be completed by the end of year 2000. Here we assume a HERA shutdown on May 1st 2000.

Timetable												
Tasks	2000											
	01	02	03	04	05	06	07	08	09	10	11	12
Magnet Constr./tests	XX	XX	XX	XX								
Installation							XX	XX			XX	XX
BPC Modifications			XX	XX	XX	XX						
Alignment										XX	XX	XX
Surveying												XX
Check-out in HERA												XX
Magnet map.(in situ)												XX
Beam Tests									XX	XX		

Timetable						
Tasks	2001					
	01	02	03	04	05	06
Magnet Constr./tests						
Installation	XX					
BPC Modifications						
Alignment						
Surveying	XX					
Check-out in HERA						
Magnet map.(in situ)	XX					
Beam Tests						

8 Final Round of Optimizations

The final position of the spectrometer will be determined by the bending dipole magnet field. The various studies in this proposal assumed an operating $\int Bdl = 0.3$ Tm and a maximum $\int Bdl > 0.36$ Tm. It is possible that the available magnet be of slightly lower $\int Bdl$. In this case new optimization studies will be performed and the spectrometer will have to be positioned farther downstream the exit window (current $z = 101.8m$).

The positioning of the spectrometer farther downstream will also eliminate any background from proton beam-halo interactions. Rates of $\simeq 5KHz$ have been measured by a pair of scintillation counters at SR93m (1m from the photon exit window) right next to the proton beam pipe (active area similar to the BPC) [12]. Such interactions occur anywhere along a proton bunch path but they can consist background only when hits in the spectrometer occur in time with hits from a bunch crossing. Since bunch crossings occur every 96nsec (28.8m photon distance), spectrometer positions Z at which proton beam-halo background is in time with good events are: $2Z/c = n96$ $nsec$, where c is the speed of light and n integer. Bad choices for the spectrometer position are 100.8 or 115.2 or 129.6 meters. Currently the spectrometer sits at 101.8 meters which is 6.7 $nsec$ close to a bad position. The BPC time resolution is 1 $nsec$. If the spectrometer is pushed 1 meter farther downstream this corresponds to a 13.3 $nsec$ difference from proton beam-halo coincidence. This time difference allows for easy rejection of the proton beam-halo background.

9 Conclusions

In this report a new technique for measuring the ZEUS luminosity was proposed. The experimental setup consists of a dipole magnet and two existing small calorimeters. The proposed luminosity spectrometer heavily relies on the planned *6 meter tagger* calorimeter. The characteristics of the spectrometer technique are summarized below:

- Small systematic errors due to pile-up. With acceptance $A \simeq 3\%$, the chances of confusion from a second photon are reduced by two orders of magnitude.
- Accurate knowledge of the acceptance ($\Delta A/A < 1\%$) in a window of width $\Delta E_\gamma \simeq 3\ GeV$, as determined with the use of the 6m tagger.
- Insensitive to synchrotron radiation even at peak luminosity.
- Small errors from energy scale uncertainty due to the good BPC resolution (single photon energy measurement resolution is of order 3-4%), absence of pile-up, and the beam energy constraint.
- The measured coincidence rates 3 KHz for $L = 10^{31} cm^{-2} s^{-1}$ allow for independent sequential measurements of the luminosity and monitoring of beam changes every few seconds.
- Good photon beam profile reconstruction at the exit window. Shifts of the profile mean values smaller than $\simeq 2mm$ can be measured every 10 seconds. The standard deviation of the profile distribution can be reconstructed with a few % uncertainty.
- The theoretical photon bremsstrahlung cross section is well understood and small in the energy range used by the spectrometer.

Our final conclusion from this study is that the listed luminosity spectrometer characteristics and expected systematic errors (table 6) make the technique much simpler and more accurate than the current luminosity measurement method, especially for high luminosity operation after the HERA upgrade.

References

[1] The HERA Luminosity Upgrade, editor U.Schneekloth, DESY HERA 98-05 July 1998.

[2] K. Piotrzkowski, *Experimental Aspects of the Luminosity Measurement in the ZEUS experiment*, Internal Report, DESY F35D-93-06, October 1993.

[3] R. Graciani, *Studies for a new electron tagger at 6 m.*, ZEUS-Note 99-038, June 1999.

[4] W. Daniluk, A. Kotarba, M.B. Przybycien, W. Wierba, *Electronics and DAQ for an Upgraded Luminosity Monitor*, ZEUS Note 99-043 03/08/99.

[5] ZEUS Luminosity Monitor Group *First Measurement of HERA Luminosity by ZEUS Lumi Monitor*, DESY 92-066, May 1992.

[6] K. Piotrzkowski and M. Zachara *Determination of the ZEUS Luminosity in 93*, ZEUS Note 94-167, January 1995;
K. Piotrzkowski and M. Zachara *Determination of the ZEUS Luminosity in 1994*, ZEUS Note 95-138, October 1995.

[7] K. Olkiewicz, A. Eskreys *Off-line Luminosity Calculation in the ZEUS experiment in 1997, 1998 and 1999*, ZEUS-Note 99-044, August 1999.

[8] H. Bethe and W. Heitler, Proc. Roy. Soc. **A146** (1934) 83.

[9] B. Surrow, *Measurement of the Proton Structure Function F_2 at Low Q^2 and Very Low x with the ZEUS Beam Pipe Calorimeter at HERA*, DESY-THESIS-1998-004, March 1998.

[10] W. R. Nelson, H. Hirayama and D. W. O. Rogers, *The EGS4 code system*, SLAC Report SLAC-265 (1985).

[11] R. Graciani, private communication (August 1999).

[12] U. Schneekloth, private communication (October 1999).